ISTANBUL TECHNICAL UNIVERSITY ★ GRADUATE SCHOOL OF SCIENCE ENGINEERING AND TECHNOLOGY

DEVELOPMENT OF A (DOPPLER-PRESERVING) DIGITAL SIGNAL PROCESSING ALGORITHM FOR A FMCW RADAR

M.Sc. THESIS

Hasan İŞEL

Department of Electronics and Telecommunication Engineering

Telecommunication Engineering Programme

SEPTEMBER 2013

ISTANBUL TECHNICAL UNIVERSITY ★ GRADUATE SCHOOL OF SCIENCE ENGINEERING AND TECHNOLOGY

DEVELOPMENT OF A (DOPPLER-PRESERVING) DIGITAL SIGNAL PROCESSING ALGORITHM FOR A FMCW RADAR

M.Sc. THESIS

Hasan İŞEL
(504111318)

Department of Electronics and Telecommunication Engineering

Telecommunication Engineering Programme

Thesis Advisor: Prof. Dr. Selçuk PAKER

SEPTEMBER 2013

İSTANBUL TEKNİK ÜNİVERSİTESİ ★ FEN BİLİMLERİ ENSTİTÜSÜ

FMCW RADAR İÇİN SAYISAL İŞARET İŞLEME ALGORİTMASI TASARIMI

YÜKSEK LİSANS TEZİ

Hasan İŞEL
(504111318)

Elektronik ve Haberleşme Mühendisliği Anabilim Dalı

Telekomünikasyon Mühendisliği Programı

Tez Danışmanı: Prof. Dr. Selçuk PAKER

EYLÜL 2013

Hasan İŞEL, a M.Sc. student of ITU Graduate School of Science Engineering and Technology 504111318 successfully defended the thesis entitled **"DEVELOPMENT OF A (DOPPLER-PRESERVING) DIGITAL SIGNAL PROCESSING ALGORITHM FOR A FMCW RADAR"**, which he/she prepared after fulfilling the requirements specified in the associated legislations, before the jury whose signatures are below.

Thesis Advisor :	**Prof. Dr. Selçuk PAKER** Istanbul Technical University	.....
Co-advisor :		.....
Jury Members :	**Prof. Dr. Sedef KENT** Istanbul Technical University	.....
	Prof. Dr. Nebiye MUSAOGLU Faculty of Civil Engineering, I.T.U.	.....
		.....

Date of Submission : **03 May 2013**
Date of Defense : **20 September 2013**

To my family,

FOREWORD

First of all, I would like to state my gratefulness to Prof. Dr. Walter Randeu, Prof. Dr. Wolfgang Bosch and Prof. Dr. Selcuk Paker giving me chance to work and Radar Team of Graz University of Technology for their technical assistance and help to sustain my works during Erasmus exchange programme.I would like to thanks to Dipl. Helmut Paulitsch for teaching and contribution my weather radar acknowledge.Finally, I want to express my appreciation to my family supporting my education and their unforgettable morality support.

September 2013

Hasan İŞEL
(Telecommunication Engineer)

TABLE OF CONTENTS

Page

ABBREVIATIONS

CW	**:** Continuous Wave
DSD	**:** Drop Size Distribution
DFT	**:** Discrete Fourier Transform
FFT	**:** Fast Fourier Transform
FMCW	**:** Frequency Modulated Continuous Wave
RCS	**:** Radar Cross Section

LIST OF TABLES

Page

LIST OF FIGURES

Page

DEVELOPMENT OF A (DOPPLER-PRESERVING) DIGITAL SIGNAL PROCESSING ALGORITHM FOR A FMCW RADAR

SUMMARY

Radar Technologies have wide range of application areas; especially for the defence industry, radar engineering has an essential position, on the other hand there are quite a lot of applications in daily life such as weather estimations and predictions, volcano activities, measurements on sky and oceans etc. Rain radar measurements are used in water management, flood forecasting and energy planning of cities or countries.

In this thesis, by developing a digital signal processing algorithm for rain form of precipitation using Frequency Modulated Continues Waves (FMCW) radar, it is aimed to observe precipitation behaviour and calculate returned signal strength of volume target, range and velocity of randomly distributed drops. Additionally, this study is a foresight for MARG - "Development of a high resolution, low cost, short range precipitation radar system" EU project.

In the designed algorithm, firstly target volume is created by considering calculation time and enabling drops to fall in antenna beam resolution volume in time. Using Marshal-Palmer drop size distribution, rain drops were created and located randomly in the volume. Then rain drops which are located in the antenna beam resolution volume were chosen and radar cross section values were calculated considering Rayleigh scattering region. Because, in the MARG project, operating frequency is determined as 5.6 GHz, and when frequency and target's size are compared, which is ten times smaller than wavelength, target falls into Rayleigh scattering region. Terminal velocity of drops were calculated by Atlas et al.'s equations which give relation drops diameter and terminal velocity.

Antenna half power beam degree was decided as 2° but antenna and the other parameters like rain rate can be determined and changed according to radar features.

By using position vector of rain drops in the antenna beam resolution and velocity, phases were determined and also by considering RCS, distance, pulse width, frequency and other related parameters, I (phase) and Q (quadrature) component of received signal were calculated. These components can be used to investigate reflectivity, velocity of targets and velocity spread. First and second Fast Fourier Transform (FFT) was implemented for range and velocity information.

All processes were carried out using Matlab. Designed algorithm allows scanning all elevation and azimuth.

FMCW saw tooth modulation (in 3 types) is used 5.6 GHz central frequency and frequency deviation is ± 1.5 MHz. Algorithm allows that investigation area is defined by user in range, elevation and azimuth and box which has margin for letting drop enters and exits from antenna radiation area in addition to specified area.

Three kind of modulation are used in the Thesis. In first type, it is being taken samples on received signal by waiting for a while which is two way travel duration between radar and target at maximum range. In other words, while radar is working, receiver starts to take samples after wave turned back from farthest target. This method helps to take same amount of samples from each drop in the all range interval (Figure 5.1). Modulation type two is eliminates also second beat frequency by waiting for a while, which is two way travel duration between radar and target at maximum range, before ramps starts. When type 2 is compared with type 1, only difference is that waiting for a while before taking samples (meanwhile transmitter process) in type 1 and in type two receiver stops working until last transmitted frequency turns back from farthest target before starting next ramp. Type 3 is unset saw tooth modulation.

FMCW RADAR İÇİN SAYISAL İŞARET İŞLEME ALGORİTMASI TASARIMI

ÖZET

Radar teknolojisi yaygın bir kullanım alanına sahiptir. Tarihsel gelişim sürecine askeri uygulamalarla başlanan radar, daha sonra kendine sivil kullanım alanlarında yer bulmuştur. 1922 ile 2. Dünya Savaşı arası yıllarda büyük bir gelişim gösteren radar, meteoroloji alanında kendine yer bulamamıştır. Amerikan ordusunda görev yapmış olan David Atlas, savaş yılları sırasında radarların yağmur gibi yağış olaylarının alıcıda gürültü olarak ortaya çıktığını farketmiştir. Savaş sırasındaki tecrübesinden çıkan fikir ile savaş sonrası ilk meteoroloji radar uygulaması David Atlas tarafından gerçekleştirilmiştir.

Meteoroloji radarları, özellikle bu tezin konusu olan yağmur olayını inceleyen sistemler insan hayatı için büyük fayda sağlamaktadır. Uzun vadede bölgelere ait yağış rejimlerinin istatistiğini belirleyerek, bölgenin tarım, temiz su, enerji planlamalarını gerçekleştirmek ve sel gibi doğal afetlerin önüne geçmek için kullanılabilmektedir. Ayrıca uydu haberleşme sisteminde, ışınım yolunu meteoroloji radarlarını kullanarak yağış sırasında anlık işaret gücünü ayarlayarak uydulardaki enerji tasarrufu sağlanabilmektedir.

Meteoroloji radar üzerine benzetimi, çıktı olarak I (in-phase) ve Q (quadrature) verilerini kullanarak çeşitli yağış durumlarında ve radar özelliklerinde meteoroloji radar işareti ve hassasiyetinin nasıl bir davranış gösterdiğini incelemeye imkan sağlamaktadır. Meteoroloji radar uygulamalarında hedeften dönen radar işareti hedefin, ki meteoroloji radarlarında hedef bir hacim içerisinde rastgele dağılmış çok sayıda elemandan oluşmaktadır, yansıtıcılığını, hızını ve hız dağılımını tahmin etmek için kullanılır. Bu değişkenleri belirleyebilmek için literatürde bir çok matematiksel ilişkiler üretilmiştir. Matematiksel denklemleri oluştururken bir çok araştırmacı Dünyanın farklı bölgelerinde çalışmalar yaparak katsayıları o yerin yağış özelliklerine göre belirlemiştir. Bu ilişkilerden biri yansıtıcılık faktörü ile yağış miktarı arasındadır. Bir çok deneysel, istatistiksel çalışma da hacim içerisindeki yağmur damlalarının yarıçaplarının dağılımını belirleyen matematiksel ilişkiyi çıkarmak için gerçekleştirilmiştir. Yağmur damlasının yarıçap dağılımını kullanarak kesin yağış miktarı, yansıtıcılık faktörü ve damlaların düşüş hızı gibi bilgileri çıkartılabilmektedir.

Tezin öncellikli amacı, bir avrupa birliği projesi olan MARG (yüksek çözünürlüklü, düşük bütçeli ve kısa erimli yağış radar sistemi) için ön görü oluşturabilmektir. Bu projede amaç frekans modülasyonlu sürekli dalga işareti kullanarak yağış sırasında geri dönen işaretin gücünü ve dolayısıyla hedefin yansıtma miktarını ölçmektir. Günümüzde meteoroloji radarları genel olarak darbe radarlarıdır. Frekans modülasyonlu sürekli dalga radarlarının en büyük avantajı üretiminin ucuz ve basit olmasıdır çünkü az enerji harcamaktadır.

Bu çalışmasında 5.6 GHz operasyon frekansında fmcw kullanarak yağmur olayını inceleyen benzetim ortamı oluşturulmuştur. Benzetim ortamı öncelikle bütün istikamet ve irtifa açılarında tarama olanağı sağlamaktadır. Hesaplama süresini kısaltmak amacıyla yağmur olayının gerçekleşeceği ortam anten ışıma örüntüsünü referans alarak oluşturulmuştur. İstikamet ve irtifa açıları değiştikçe ortam da değişime göre konum almaktadır. Gözlem kübü ve antenin yarı güç ışıma açısını kullanarak oluşturulan ışıma örüntü alanı berlirledikten sonra yağmur damlaları Marshall-Palmer yağmur damlası yarı çapı dağılımı denklemine göre oluşturulmuştur. Doğada küçük boyutta yağmur damlaları (0.35mm − 1mm) daha fazla bulunurken büyük damlalar (1mm−5mm) daha az bulunmakta ve 5mm − 8mm arası çapa sahip olan damlalar ise düşüş sırasında parçalanarak daha küçük damlalar oluşturmaktadırlar. Bu davranışa göre yağmur damlaları oluşturulurken küçük damlaların sayısı fazla tutulmuştur. 0.5mm ile 1mm arası damlalar 0.08 çözünürlük ile 1mm ile 5mm arası damlalar 0.3 çözünürlük ile ve son olarak 5mm ile 8mm arası damlarlar 0.8 çözünürlük ile üretilmiştir. Yağmur damlalarının yarıçaplardaki sayısı exponansiyel bir ifade olan Marshall-Palmer denklemi kullanarak belirlenmiştir. Yağmur damlaları belirlendikten sonra, gözlem kübü içerisinde rastgele yerleştirilmiş ve elde olan kartezyen koordinatları küresel koordinata çevirerek bir matrise kaydedilmiştir.

Daha sonra radar kesit alanını (RCS) her yağmur damlası için hesaplanmıştır. Çalışma frekansı ile hedefin boyutları karşılaştırıldığında geri saçılım Rayleigh dağılımı içerisinde kalmakta ve uygun denklem kullanarak RCS değeri hesaplanmış ve koordinat bilgisini içeren matrise kaydedilmiştir.

Bir sonraki adımda anten ışıma alanına giren yağmur damlaları belirlenmiş ve bir matriste çap, koordinat ve RCS değerleri kaydedilmiştir. Bu veriler kullanarak I ve Q değerleri hesaplanmış ve I+jQ değerleri bir matrise kaydedilmiştir. Daha sonra algoritma yeniden konumlandırma işlevini kullanarak yerçekimi ve rüzgar etkisiyle oluşan konum değiştirme gerçekleştirilmiş yeniden anten ışıma alanına giren yağmur damlaları belirlenip aynı işlemler tekrarlanmıştır.

Modülasyon tipi olarak testere dişi tercih edilmiştir. Testere dişi bir birini izleyen frekans zaman değişimindeki rampalardan oluşmaktadır. Periyodik olarak bir birini izleyen rampa dizileri ise bazı problemler yaratmaktadır. FMCW radar tekniğinde gelen dalga zaman ve frekans değişkeninde ötelenmektedir hedefin hareketine konumuna bağlı olarak. Gelen dalga ötelenmiş bir şekilde gelerek, alınan işaret ile çarpılarak fark frekansı elde edilir. Rampa geçişleri sırasında bir önceki rampanın gönderdiği dalgaların bir kısmı bir sonraki rampa başladıktan sonra radara ulaşmaktadır. Bu durumda ise ilk rampadan çıkanlar karıştırıcıda bir sonraki rampada olan gönderilen işaret ile çarpılmaktadır. Bu durum ise istenmeyen negatif ikinci bir fark frekansı oluşturmaktadır. Bu problemi gidermek için iki çeşit yöntem denenmiştir.

Bu çalışmada üç farklı modulasyon tipi kullanılmıştır, bunlardan ikisi ise istenmeyen negatif ikinci fark frekansını elemenmesi için kullanılmıştır. Üçüncü tip modulasyon testere dişidir. Birinci tip modulasyon, rampa başlangıcından sonra gönderilen dalganın en uzak noktadaki hedefe ulaşıp, radar dönmesi arasında geçen süre kadar zaman geçtikten sonra örnek almaya başlanılmasıdır. Bu sayede her hedeften alınan örnek sayısının eşit tutulması ve istenmeyen negatif ikinci fark frekansından kurtulunmasıdır. İkinci tip modulasyonda ise bir sonraki rampa, dalganın en uzak hedefe varıp geri dönmesi kadar geçen süre sonra başlatılmasıdır. Birinci tip modulasyonda periyodik rampalar normal çalışırken sadece örnek alınma

zamanları ayarlanmış olup, ikinci tipte ise rampalar arası bekleme süreleri konmuştur. Modulasyon tiplerinin etkilerini gözlemlemek için yakından uzağa olmak üzere aynı hıza sahip dört adet hedef kullanılmıştır. Birinci ve ikinci tip modulasyonlar istenmeyen ikinci fark frekansı problemini gidermiş ve birinci tipte ise 2D FFT genlikler üzerinde de gelişme gözlenmiştir.

İşlemin gerçekleştirildiği gözlem alanı ve modulasyon tipi kullanıcı tarafından belirlenebilmektedir. Kullanıcı menzili ve anten yarı güç örüntü açısı dahilinde bir açı belirleyerek gözlem alanı ayarlanır. Kullanıcının belirlediği alana ek olarak bir marjin program tarafından eklenmektedir. Bu marjin yağmur damlalarının anten ışıma alanına girmesi ve çıkması için alan sağlamaktadır. Zaman içerisinde yağmur damlaları belirlenen gözlem küpünde rüzgar ve yer çekimi sebebiyle oluşan hızları ile orantılı olarak konum değiştirmektedirler. Anten ışıma alanına giren yağmur damlalarından geri dönen işaretler ise işlenmektedir.

Yapılan çalışmada modülasyon tiplerindeki değişimin etkileri gözlemlenmiştir. Üçüncü tip modülasyonda rampalar arası geçişlerde istenmeyen ikinci fark frekansı oluşmaktadır. Bu ise menzil − Doppler grafiğinde gürültülere yani yan lobların yüksek değerlerde çıkmasına neden olmaktadır. İkinci ve üçüncü tip modülasyonlarda frekans − zaman rampasındaki değişiklerle ikinci fark frekansının oluştuğu zamanlar yok edilmiş ve etkileri grafiklerde gözlemlenmiştir.

Modülasyon etkilerinin yanı sıra algoritmanın hedefleri ve Doppler hızları kestirimi de incelenmiştir. İlk olarak on adet hedef kullanılarak menzil ölçümü yapılmıştır. Grafik ve tablo üzerinde sonuçlar derlenmiştir. Gerçek konum değerleri ve işaret işleme sürecindeki sonuçlar tabloda karşılaştırılmıştır. Sonuçlarda ise band genişliğine bağlı olan çözünürlük etkisi de görülebilmektedir. Aynı işlem Doppler hızı kestirimi için de gerçekleştirilmiştir. Doppler işlemi sonuçları da tabloda derlenmiş ve karşılaştırmalar yapılmıştır. Rampa sayısına bağlı olan çözünürlük etkisi de sonuçlarda görülebilmektedir. Bir sonraki işlemde bilgisayar kabiliyeti de gözetilerek beş yüz adet hedef kullanılarak bir yağmur olayının grafiklere nasıl yansıdığı menzil − Doppler grafiği ile gösterilmiştir. Hedef sayısındaki artış sonuçlara gürültü tarzı bir etki oluşturduğu gösterilmiştir.

1. INTRODUCTION

Radar Technologies have wide range of application areas. Defence industry is very important in radar engineering due to the ongoing projects, on the other hand there are quite lot applications in civil life like weather estimations and predictions, volcano activities, measurements on sky and oceans etc.

Weather radars have an important place in modern daily life. Weather radars make it possible to measure precipitation in the air much more accurately and make qualified forecast by keeping statistics about precipitation history. Besides, it is possible to make observation and keep statistical data not only for local weather reports but also for water management, disaster control, energy planning and so forth.

Using I and Q components which represent the received signal, reflectivity factor of distributed targets in the volume and velocity of targets and velocity spread can be estimated. Reflectivity can be used to estimate rain rates. In the literature, there are significant amount of works which describe relation between reflectivity and rain rates. Furthermore, there are equations are formed by empirically for calculating terminal velocity of drops and drop size distribution in the volume and rain drop sizes can be determined by using different methods like 2-D video disdrometer.

The simulator is based on calculation of returned signal strength from each drop in the resolution volume. It allows making a scan in required elevation and azimuth. Marshal-Palmer drop size distribution is used for creating drops in the volume and located randomly. Terminal velocities are determined by using Atlas et al.'s equations which has drop sizes as a parameter. Additionally, wind speed factor is considered as effect on replacement. Radar signal processing produces an output consisting drop's velocities and range information by using first FFT and second FFT. Moreover, reflectivity, rain rates and received signal strength can be calculated.

1.1 Purpose of Thesis

While Pulse Doppler Radar operation principle relies on traveling time difference between transmitter and target to obtain range and velocity information; in frequency modulated continuous wave (FMCW) radar, distance info is a parameter of frequency shift. Difference frequency between echo and transmitted wave is called beat frequency which is accrued by moving targets. Also, frequency modulator function (e.g. triangle) is important to determine velocity of the targets simultaneously with distance information.

The reason of choosing FMCW technique instead of pulse radar is that FMCW radar has advantages on power consumption and high resolution for ranging and velocity. However, it requires signal processing capabilities and spectral analysis (DFT, FFT - Discrete Fourier Transformation, Fast Fourier Transformation) on echo signal having different frequencies. Especially operation on the distributed targets like weather events require more complex process on received signal which has power being calculated separately for each range gate over a wide range. In the thesis, I and Q formulation, which is adopted for the pulse radar precipitation simulation by Capsoni and D'Amico, is combined with FMCW radar process and full azimuth and elevation environment scanning by 2D FFT spectral analysis which is proposed by Barrick [3] for FMCW radar signal process to extract Doppler and range map. The main goal of this study is to find a processing/modulation scheme that allows solving Doppler and ranging ambiguities.

1.2 Related Works

In the literature, precipitation simulators are focused on Doppler pulse radar. Capsoni and D'Amico [4] described physical simulator by adopting Doviak and Zrinc's [5] I and Q formulism;

$$I(t_s, T_s) = H \sum_i \left(\frac{\sqrt{(\sigma_i)} I_i |W_i|}{r_i^2} f(\theta_i, \varphi_i) \cos(\gamma_i) \right) \tag{1.1}$$

$$Q(t_s, T_s) = H \sum_i \left(\frac{\sqrt{(\sigma_i)} I_i |W_i|}{r_i^2} f(\theta_i, \varphi_i) \sin(\gamma_i) \right) \tag{1.2}$$

where

$$\gamma_i = (\frac{4\pi r_i}{\lambda}) + (\frac{4\pi v_i T_s}{\lambda}) - \varphi_i - \beta_i \tag{1.3}$$

and

$$H = \sqrt{\frac{P_t G^2 \lambda^2}{(4\pi)^3}} \tag{1.4}$$

P_t is the transmitted peak power, (r_i, θ_i, ϕ_i) are the coordinates of the i^th scatterer, G is the antenna gain, λ is the wavelength, li is the extra attenuation due to rain and gases in the path toward and from the radar bin, W_i is the so-called range weighting function (RWF), $f(\theta_i, \phi_i)$ is the antenna directivity function (power), σ_i is the back-scattering cross section of the i^th scatterer, v_i is the projection of the scatterer velocity along the radar direction, φ_i is the phase contribution due to the scattering function, and β_i is the phase contribution due to the RWF, the antenna directivity pattern, and the propagation path. In this thesis, RWF is not used because for FMCW, RWF is an unnecessary parameter.

In 2005, Ulf P. Schroder [6] wrote a thesis on weather signal simulator which gives information about creating simulation environment while developing a simulator in Matlab. Doviak and Zrinc's [5] book which is called "Doppler Radar and Weather Observation" is very helpful to understand theory, aspects of weather radar. Barrick [3] proposed double Fast Fourier Transform (FFT) process to obtain range and Doppler results. First FFT gives result for range and second FFT over matrix which is acquired by first FFT is for Doppler. Detailed explanations are in the following chapters.

1.3 Thesis Outline

In Chapter two, weather radar and rain theory is explained. Basic radar principle and parameters like range, antenna and radar equation are mentioned. Weather radar equation, scattering regimes for precipitation and reflectivity factor, which is very important parameter, are explained. Also, physics of precipitation is summarized by mentioning about rain drop size, drop size distribution, terminal velocity of drops and rainfall rate.

In Chapter three, continuous wave radars and frequency modulated continuous waves are described and some important points are emphasized. Idea of I (in-phase) and Q (quadrature phase) components, which are output values of the system, are clarified.

Also for the FMCW radar signal processing and FFT windowing process are explained with some design considerations.

In Chapter four, simulation algorithm flow is mentioned in details by considering the results from MATLAB. Modulation types which are for eliminating negative unwanted second beat frequency and improving FFT results amplitudes. For different number of drop and modulation types, results are shown in the Figures and explained.

2. WEATHER RADAR AND RAIN THEORY

2.1 Radar Principle

Radar (Radio Detection and Ranging) theory is based on sensing reflected electromagnetic waves and analyzing differences between transmitted and received signals to obtain information about the targets. It was the first time when reflected signals from dielectric objects were analyzed and the effects of the objects were determined by Heinrich Hertz at the end of 19th century. However, progression of radar technology was not fast until 1922. First successful experiment was carried out by US Naval Research Laboratory by detecting wooden ship using 600MHz signal. In the following years, radar research became more popular in some countries like USA, England and France [7]. After Second World War, modern radar technology have been used widely for air traffic control, astronomy, military defence systems, controlling ship traffic, geological observations and weather forecasting.

2.1.1 Radar range and Doppler shift

adar range is related with traveling time of signal from transmitter antenna to target and from target to receiver antenna. Electromagnetic waves travel at speed of light which is symbolized with "c" and equals to $3 * 10^8 m/s$. Range is;

$$R = \frac{c * T}{2} \tag{2.1}$$

T is the traveling time. This traveling time for the pulse radars is related to the time between two pulses in unambiguous situation. This time period T_{pr} is called pulse repetition period and maximum range;

$$R = \frac{c * T_{pr}}{2} \tag{2.2}$$

Doppler Effect is shifting on center frequency due to target movements relative to source. Radial component of the velocity determines Doppler shift;

$$R = -\frac{2v_r}{\lambda} \tag{2.3}$$

First effect is on the way to target and second effect is reflected signals way to radar.

2.1.2 Radar range equation

Radar range equation is used to calculate received signal power. Firstly, electromagnetic waves radiate from antenna and travel to target. Then, waves reflect on the target's surface. Reflected signal power is related to shape of target which is defined with Radar Cross Section (RCS). RCS is the ratio of reflected and incident power density, σ.

At the receiver point, power density can be given;

$$P = \frac{P_t * G}{4\pi r^2} * \frac{\sigma}{4\pi R^2} [W/m^2] \tag{2.4}$$

Range of antenna is related with effective area (A_eff) of antenna;

$$A_eff = \frac{G\lambda^2}{4\pi} [m^2] \tag{2.5}$$

$$P_rec = \frac{P_t * G}{4\pi r^2} * \frac{\sigma}{4\pi R^2} * A_eff \tag{2.6}$$

And by taking losses factor into account, received power can be expressed;

$$P_{rec} = \frac{P_t G_r G_t \sigma \lambda^2}{4\pi^3 R^4 L} \tag{2.7}$$

L: one way loss term due to components, elements and absorption in the atmosphere
λ: operating wavelength

According to equation 2.7, received power is connected with range, operating frequency, radar cross section and radar's technical features such as antenna and transmitted power.

2.2 Weather Radar

Weather radar is a type of radar that has been used to locate precipitation, observe motion of distributed targets and determine its type. The idea of using the radar technology for weather observation has come up by realizing noise effects of rain,

snow etc. during Second World War. First, implemented weather radar was developed by David Atlas in USA.

Modern weather radar systems are mostly pulse-Doppler radars, but in recent years frequency modulated continuous wave radars have also became a good option to reduce system cost and increase resolution in long distance measurements.

2.2.1 Weather radar range equation

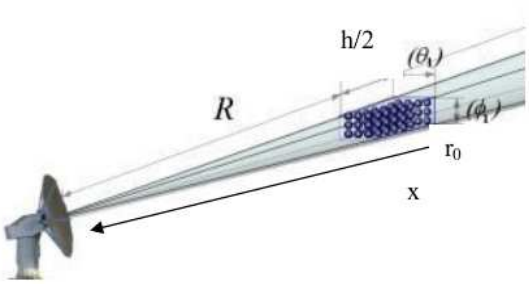

Figure 2.1: Volume Target .

First of all, there is one target in equation 2.7 however for the precipitation, it is better to indicate backscatter radar cross section $\eta(m^2/m^3)$ in volume [8] (Figure: 2.1).

$$\eta(r_i,\theta_i,\phi_i) = \lim_{V\to 0} \frac{\sigma(r_i,\theta_i,\phi_i)}{V} \tag{2.8}$$

V: Volume of targets

σ: Radar cross section

Power density at target:

$$S_{inc}(r,\theta,\phi) = \frac{P_t G(\theta,\phi)}{4\pi r^2} \tag{2.9}$$

$$t_e = \frac{2}{c}(r_0 - r) \tag{2.10}$$

$$(r_0 - r) = x \tag{2.11}$$

Reflected power from differential target volume;

$$dP_r ef = S_{inc}\sigma \tag{2.12}$$

$$dP_{ref} = S_{inc}\eta dV = S_{inc}\eta(r,\theta,\phi)r^2\sin\phi dr d\theta d\phi \tag{2.13}$$

Received signal at the receiver stage;

$$dP_r = \frac{dP_{ref}A_{eff}(\theta,\phi)}{4\pi r^2} = \frac{\lambda^2}{4\pi}\frac{dP_{ref}G(\theta,\phi)}{4\pi r^2}, \tag{2.14a}$$

$$dP_r = \frac{dP_t G^2(\theta,\phi)\eta(r,\theta,\phi)\sin\phi dr d\theta d\phi\lambda^2}{4\pi^3 r^2}, \tag{2.14b}$$

After integrating in the volume, in the condition of $h \ll r_0, 1/r^2\ 1/{r_0}^2$ and

$$P_r = P_t\tau\frac{{G_{max}}^2\lambda^2 c(\Delta\theta_{3db})^2}{1024\ln 2\pi^2{r_0}^2 L}\eta \tag{2.15}$$

With antenna half power beam width;

$$\int_{\phi=0}^{\pi} G^2(\phi)\sin\phi d\phi \sim {G_{max}}^2\frac{(\Delta\theta_{3db})^2}{16\ln 2} \tag{2.16}$$

$\Delta\theta_{3db} = Half\,power\,beam\,width = \Delta\theta_{V3db} = \Delta\theta_{H3db}$

L=Loss factor due to components, elements and absorption in the atmosphere

2.2.2 Scattering

Reflection of electromagnetic waves from target is directly related with backscatter cross section. As it is mentioned before, backscatter cross section is;

$$\sigma = \frac{reflected\,power\,density\,towards\,source}{incident\,power\,density} = \log_{R\to\infty} 4\pi r^2\frac{|E_r|^2}{|E_i|^2} \tag{2.17}$$

Where r is distance between radar and target E_r =reflected field strength E_i = field of incident strength Backscatter cross section is also related with wavelength of the operation frequency and size of target. According to ratio of wavelength and size, there are three scattering regions. If ratio is equal to$2\pi a/\lambda << 1$, it is called Rayleigh region, else if ratio is equal to $1 < 2\pi a/\lambda < 10$, it is Mie region and in the situation of $10 < 2\pi a/\lambda$, it is optical region [7] (Figure 2.3).

In thesis, scattering region is in Rayleigh region because operation frequency is 5.6 GHz and when compared to rain drops, ratio is less than 1.

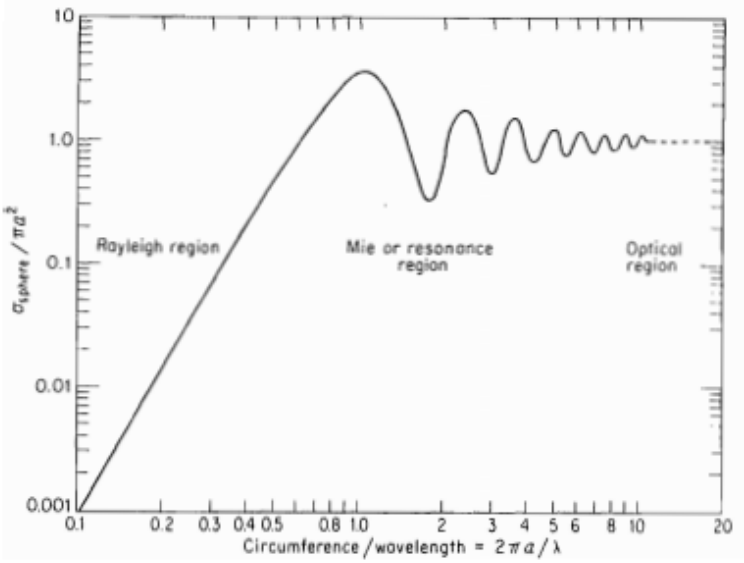

Figure 2.2: Scattering Region.

For the rain drops, Rayleigh backscatter cross section can be written according to backscattering efficiency [9];

$$Q_b = 4x^2 \frac{|}{(\varepsilon - 1)}(\varepsilon + 2)|^2 \tag{2.18}$$

$$\sigma_b = \frac{D^2\pi}{4} Q_b(D) = \frac{\pi^5}{\lambda^4} 4x^2 |\frac{(\varepsilon - 1)}{(\varepsilon + 2)}|^2 = \frac{\pi^5}{\lambda^4} |K|^2 D^6 \tag{2.19}$$

Where, ε is the complex dielectric constant of water. $|K|^2$ is 0, 93 for water and 0,176 for ice.

2.2.3 Reflectivity factor

In weather radars, scanning radars yield to maps of reflectivity factor (Z). Radar reflectivity can be used to estimate rain rate (R) and water content (W). In the literature, there are many researches to determine statistical relation between reflectivity factor, rain rate and water content. In this thesis, water content is not a focus of interest, but according to Hagen and Yuter's [10] study, determined and recommended relationship is $W = 3.4 * Z^{4/7}$. The relation between rain rate and reflectivity is mentioned in the following parts.

Radar reflectivity factor's relation with RCS density;

$$\bar{\eta} = \frac{\pi^5}{\lambda^4}|K|^2 Z \tag{2.20}$$

And radar reflectivity is equal to the ratio of sum of rain drops diameter's sixth power and volume;

$$\bar{\eta} = \frac{1}{\Delta V}\Sigma_{i\varepsilon V} {D_i}^6 \tag{2.21}$$

The other way to calculate Z is integration of rain drop diameter in the volume by using DSD which is mentioned in the section 2.3.2;

$$Z = \int_{\phi=0}^{D_{max}} N(D) D^6 dD \tag{2.22}$$

N(D) is continuous distribution of drop sizes with diameter density. By considering weather radar equation 2.15, radar reflectivity factor is;

$$\hat{Z} = \bar{P_{rec}} \frac{1024 \ln 2 {r_0}^2 L \lambda^2}{P_t \tau {G_{max}}^2 c(\Delta\theta_{3db}) \pi^2 ?^3 |K^2|} [mm^6/m^3] \tag{2.23}$$

2.3 Precipitation Physics

2.3.1 Rain drop size and shape

Methods like 2-D video disdrometer give a chance to observe rain drop sizes and shapes. Drop diameter varies between 0.5mm and 7mm however bigger drops than 4-5mm tend to split because of movement effects during free fall in the air. Drop diameter D<0.35mm has spherical geometry, up to 1mm oblate spheroid and larger drops have flattened and drops with D>4mm concave base [5]. So, equivalent drop diameters are used.

Some statistical equations are available in the literature on horizontal and vertical radius. One of these is generated by Pruppache and Beard [11];

$$\frac{b}{a} = 1.03 - 0.124 * D/2 \tag{2.24}$$

where D is drop diameter.

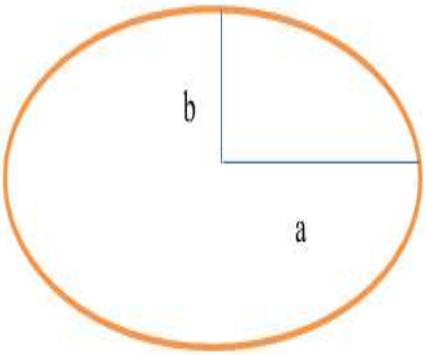

Figure 2.3: Drop Shapes.

2.3.2 Drop size distribution

Drop size distribution (DSD) is the volume density of drops per unit drop diameter and it is an essential parameter for determining reflectivity factor Z, liquid water content M and rain rate R. In the literature, there are empirical models based on observations and diameter of drops which is used as parameter of mathematical expressions, N(D). Gamma, exponential, log-normal distribution, constrained gamma distributions are available which can be suited for different region's precipitation features [12]. In this thesis, the empirically derived exponential distribution is used.

Exponential distribution is;

$$N(D) = N_0 e^{-\Lambda D} \tag{2.25}$$

where Marshall-Palmer data are;

$$\Lambda = 4.1 R^{-0.21} mm^{-1} \tag{2.26}$$

$$N_0 = 8 * 10^3 m^{-3} mm^{-1} \tag{2.27}$$

where R is rain rate in millimetre per hour.

DSD mathematical expression is required to define minimum and maximum drop diameter D because the relation between radar reflectivity factor and rain rate, it is assumed that drop sizes diverge to infinite values and it is not realistic. Therefore, the exponential drop size distribution is truncated at $D = D_{max}$ [5]. As suggested for relation with reflectivity factor, truncated drop size distribution equation is;

Table 2.1: DSD parameter values.

Kind	$N_0 mm^{-1} m^{-3}$	D_0 mm
Drizzle	30 000	$0.64R^0.21$
Country Rain	8 000	$0.9R^0.21$
Tropic Rain	14 bil.	$1.22R^0.21$

$$N(D) = \{ \begin{matrix} N_0 e^{-\Lambda D} & D_{max} < D \\ 0 & D_{max} < D \end{matrix} \quad \textbf{(2.28)}$$

For the different kind of precipitation, DSD is showed in table 2.1.

2.3.3 Terminal velocity of drops

Terminal velocity of drops depends on diameter of drops. An equation for terminal velocity, which has been commonly used, is determined by Atlas et al. [13];

$$V(D) = 9.65 - 10.3e^{(} - 0.6D)[m/s] \quad \textbf{(2.29)}$$

where D is in mm,

$$V(D) \approx 386.6D^0.67m/s[m/s] \quad \textbf{(2.30)}$$

where D is in m.

2.3.4 Terminal velocity of drops

Rain rate is an important parameter in precipitation. It is essential to keep statistics of precipitation rate for environmental planning, observing climate changes, managing the fresh water and energy etc.

Rainfall Rate can be derived from drop size distribution and velocity data.

$$R = 0.610^{-3} \int_{D=0}^{D_max} D^3 v(D) N(D) dD[mm/hr] \quad \textbf{(2.31)}$$

where D is $[mm]$, v(D)[m/s] and N(D)$[1/(mmm3)]$.

There is another significant relation between rain rate and radar reflectivity. In the literature, there are significant works to determine this relation and empirically equations are available in the form of $Z = A * R^B$. This relation has significant variation

according to precipitation's season and geographical features. For further information, [14] can be researched. In thesis commonly used Marshall-Palmer (MP) relationship is preferred,

$$Z = 200R^{1}.6[mm^{6}/m^{3}] \quad \textbf{(2.32)}$$

3. FREQUENCY MODULATED CONTINUOUS WAVES

3.1 Continuous Wave Radar

Continuous wave (CW) radars transmit continuous wave energy and receive reflected wave from target in single operation frequency. The point is that CW radars are based on Doppler Effect. The Doppler Effect changes frequency of waves by moving target relatively to transmitter. Also, these kinds of radars are called unmodulated continuous wave radars. By using Doppler information, velocity of the target can be calculated but there is no chance to determine target distance. The cost of CW radar is very low because of less complicity and also is used with sport competitions, traffic control etc.

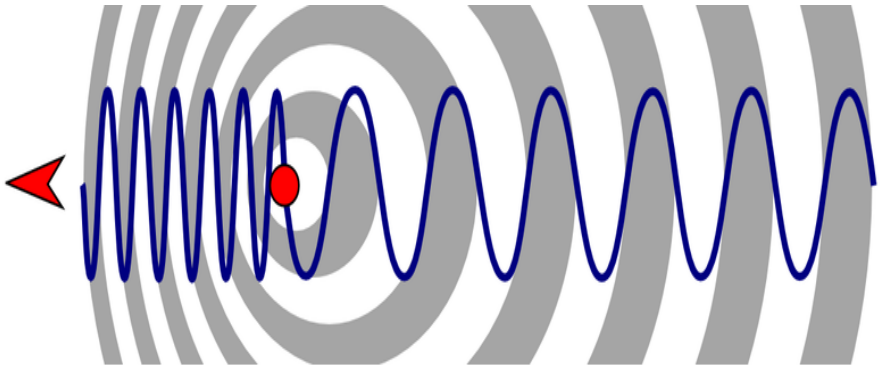

Figure 3.1: Doppler Effect by moving target [2].

3.2 Frequency Modulated Continuous Wave

Frequency modulated continuous wave (FMCW) radars are capable to determine target's distance and velocity by using frequency changes periodically in time. FMCW signal is transmitted by antenna and echo signal reflected from target is received by antenna. Then, by mixing received and transmitted signals, having different frequency due to moving targets, beat frequency, which has been used for digital signal process, is achieved.

Figure 3.2 shows principle of FMCW radar. Signal generator generates modulated signal. Before antenna, generated modulated signal is divided into two to obtain local oscillator input signal for mixer to be mixed with received signal which has difference

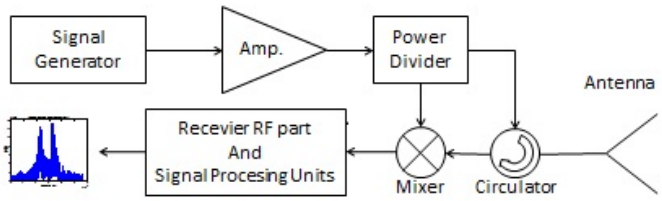

Figure 3.2: FMCW radar block diagram.

in frequency, phase and power because of moving target. After mixing, beat frequency (frequency differences between transmitted and received signal) is achieved. By using beat frequency, range and Doppler process can be started in the signal processing units.

Analytically, the transmit signal can be written;

$$V_T(t) = \cos(2f_c t + Bf_r t^2) = \cos(\varphi_t(t)) \tag{3.1}$$

Where if $fr = 1/Tr$ is sweep duration, B is bandwidth, f_c is carrier frequency.

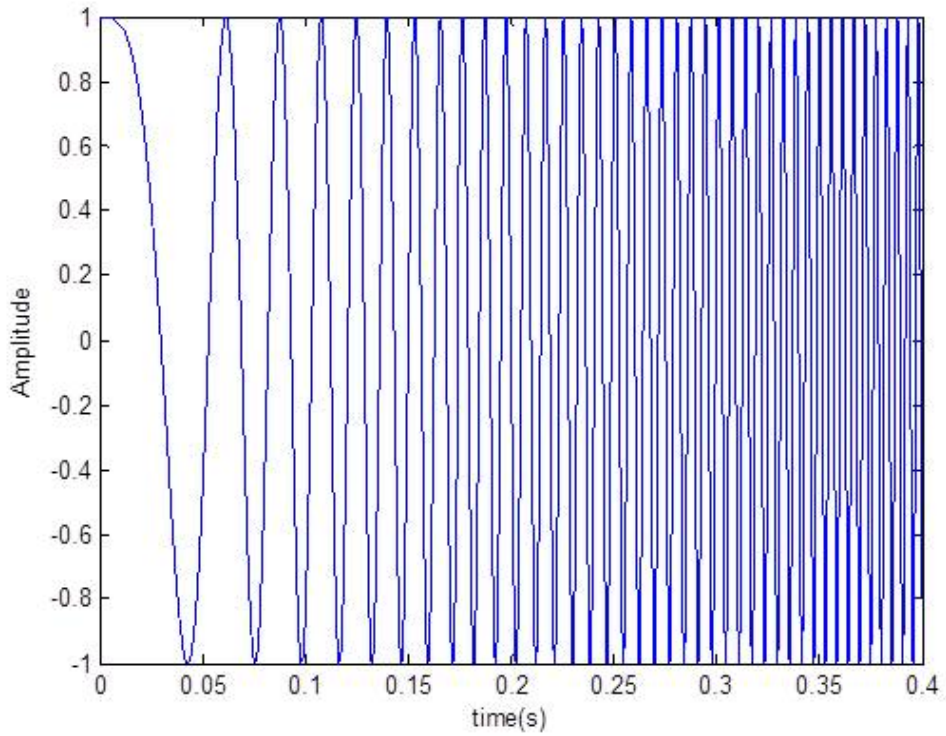

Figure 3.3: Time dependency FMCW radar transmit signal.

Frequency can be determined from derivation of phase component;

$$f_t(t) = \frac{1}{2\pi}\frac{d\varphi_T(t)}{dt} = f_c + Bf_r t \tag{3.2}$$

where B is $fmax - fmin$.

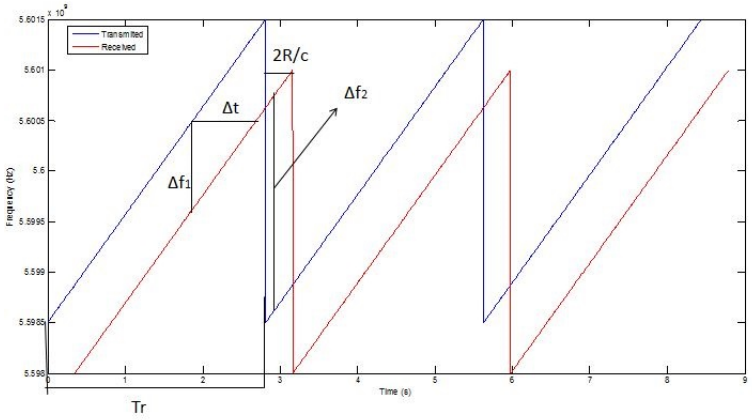

Figure 3.4: Received and transmitted signals in frequency and time.

In figure 3.5, there is a point that (Δf_2) frequency is different than the (Δf_1) beat frequency. While passing from one sweep to another sweep, when one target is considered, there is a time difference equal to $2R/c(T_r)$ where c is light velocity and R is range. When the system pass through mixer, where transmitted and received signal are mixed, second beat frequency (Δf_2) take place. If second beat frequency is higher than first beat frequency, it can be suppressed by filter. Also by choosing suitable modulation type, this problem can be removed.

Received signal can be written time dependency which is shifted version of transmitted signal in time and frequency;

$$V_R(t) = AV_T(t - t_d) = \cos(2f_c(t - t_d) + \pi Bf_r(t - t_d)^2) \tag{3.3}$$

At output of mixer, frequency difference (Δf_1) is derivation of φ_1 which is difference between transmitted phase and received phase.

$$\Delta f_1 = \frac{1}{2\pi}\frac{d\varphi_1}{dt} = \frac{2f_c v}{c} + \frac{2Br_0}{cT_r} + \frac{2Bm}{c} + \ldots \tag{3.4}$$

Where r_0 is range at $t = 0$ and m is mth sweep. In equation above, just first three terms are significant, so rest of terms aren't written. The first term is Doppler shift, second

term represents the initial range and third one is due to the accumulated range up to time mTr ([5]).

3.3 In-Phase and Quadrature Phase Components

In the assumption of one target, received signal voltage replicating the transmitted waveform of electric field E is proportional to it;

$$V(t,r) = Aexp[j2\pi f(t - \frac{2r}{c} + j\varphi]U(t - \frac{2r}{c}) \tag{3.5}$$

where U is 1 in the interval of 0 and T, otherwise 0.

and total phase is

$$\beta = 2\pi f(t - \frac{2r}{c}) + \varphi \tag{3.6}$$

By applying 90° phase shift, we can produce real and imaginary components of phase data which are respectively in phase and quadrature.

$$I(t) = (|A|/\sqrt{2})U(t - \frac{2r}{c})\cos(\frac{4\pi r}{\lambda} + \varphi + \varphi_i), \tag{3.7a}$$

$$Q(t) = (|A|/\sqrt{2})U(t - \frac{2r}{c})\sin(\frac{4\pi r}{\lambda} + \varphi + \varphi_i), \tag{3.7b}$$

Square root of the sum of I^2 and Q^2 equals to the input power and $arctan(Q/I)$ gives phase. For the stationary target, phase is equal to $\gamma = 4\pi r/\lambda + \varphi$ and if the target has movement in time, phase decreases and changes amount gives Doppler shift;

$$\frac{d\gamma}{dt} = \frac{4\pi dr}{\lambda dt}) = -\frac{4\pi}{\lambda}\upsilon_r = w_d \tag{3.8}$$

In the literature, simulators for precipitation are focused on Doppler pulse radar. Capsoni and D'Amico [4] described physical simulator by adopting Doviak and Zrinc's [5] I and Q formulism;

$$I(t_s, T_s) = H\sum_i (\frac{\sqrt{(\sigma_i)}I_i|W_i|}{r_i^2} f(\theta_i, \varphi_i)\cos(\gamma_i)) \tag{3.9}$$

$$Q(t_s, T_s) = H \sum_i \left(\frac{\sqrt{(\sigma_i) I_i |W_i|}}{r_i^2} f(\theta_i, \varphi_i) \sin(\gamma_i)\right) \tag{3.10}$$

where

$$\gamma_i = \left(\frac{4\pi r_i}{\lambda}\right) + \left(\frac{4\pi v_i T_s}{\lambda}\right) - \varphi_i - \beta_i \tag{3.11}$$

and

$$H = \sqrt{\frac{P_t G^2 \lambda^2}{(4\pi)^3}} \tag{3.12}$$

P_t is the transmitted peak power, (r_i, θ_i, ϕ_i) are the coordinates of the $i^t h$ scatterer, G is the antenna gain, λ is the wavelength, li is the extra attenuation due to rain and gases in the path toward and from the radar bin, W_i is the so-called range weighting function (RWF), $f(\theta_i, \phi_i)$ is the antenna directivity function (power), σ_i is the back-scattering cross section of the $i^t h$ scatterer, v_i is the projection of the scatterer velocity along the radar direction, φ_i is the phase contribution due to the scattering function, and β_i is the phase contribution due to the RWF, the antenna directivity pattern, and the propagation path. In the thesis, W_i and phase contributions of φ_i,β_i are ignored.

3.4 Radar Signal Processing

Pulse - Doppler radars use unmodulated pulse signals. In other words, modulation is a periodic sequence of rectangular pulses. Per time unit, number of pulses is described by Pulse Repetition Frequency (PRF). PRF bounds maximum expected Doppler frequency, so the Doppler frequency must be lower than PRF. For the Doppler signal processing, mainly two methods are used, Pulse Pair Process which is faster and Spectral Process (FFT) which makes use of the fact that the complex autocorrelation function of the received signal. FFT on complex time series is generally used to obtain an estimate of the Doppler spectrum from which the mean velocity and spectrum variance can be obtained [15]. However, in FMCW, signal processing is only performed in frequency domain. The main difference is that pulse-pair process measure phase differences. In the pulse pair process, two pulses give phase difference information in short time, hence it requires duration of process is very short. However FFT process in the long time observation requires significant processing duration. In addition, there is no decorrelation problem in the pulse pair process like FFT process because progress in the short time means that changes in the target side is very low, which means rain drops' location almost constant. Moreover, when technical part is

considered, Doppler frequency is very low compared to transmitted signal, so phase comparison is an easier way to carry out than frequency comparison.

By using double Fast Fourier Transform (FFT), target's range (time delay) and Doppler (velocity) can be examined. First Fast Fourier transform is implemented over one pulse repetition period T_r which is one sweep to achieve target range. Then, second Fourier transform is applied over several pulses to get Doppler.

For the first Fourier Transform process M times sampling has to be performed within the time period T_r. M/T_r must be minimum twice value of $2(\Delta f_1)$ which is maximum expected value of (Δf_1) according to Nyquist Theorem and (Δf_1) ;

$$(\Delta f_1) = \frac{2v}{c} f_c + B f_r t_0 + \frac{2v}{c} B \tag{3.13}$$

After first n times application FFT bounded with N value, $M/2$ range bins are procured and in the condition of Doppler term $(2v/c)fc$ is low compared range term, $Bf_r t_0$. In other words, the first FFT process on M samples within one pulse gives M/2 range bins and range bins are stored in a matrix (M/2 by N). Columns of the matrix present range bins. As an example, for the radar has maximum range of 150 km and target is at 15 km then target appears at tenth bin in the $M/2 = 100$ range bins.

The second FFT is performed over each columns (range bins). All elements in the matrix are complex because phase and beat frequency change from sweep to sweep. Target appears at Doppler frequency bins $f = (2v/c)f_c$, where f_c carrier frequency, v is velocity and c is speed of light. [3] can be read for further and detailed reading.

Here is a design consideration for FMCW radar system which is suggested by Barrick [3];

1- $B = c/(2\Delta R)$, where B is bandwidth, ΔR is range resolution desired in meter.

2- $T_r = 1/f_r$ where $f_r = 2f_{DM}$, f_{DM} is maximum target Doppler shift, $f_{DM} = (2v_m/c)f_c$ and v_m is expected maximum target velocity.

3- $N = T_c/T_r$, where T_c is the total coherent integration time is the reciprocal of desired Doppler resolution Δf_D, where $\Delta f_D = (2\Delta v/c)f_c$.

4- $M = 2R_w/\Delta R$ samples per pulse interval, T_r.

And also following situations are for checking whether optimum processing gain will be realized.

1- $\frac{1}{2}BT_r(\frac{2V_m}{c})^2N^2 \ll 1$,

2- $B\frac{2V_m}{c}\frac{2R_w}{c}N \ll 1$,

3- $B\frac{2V_m}{c}\frac{T_r}{4} \ll 1$,

4- $V_mNT_r \ll \Delta R$,

5- $\frac{dv}{dt}NT_r < \Delta v$.

3.5 FFT Windowing

While FFT process, which is a periodic function, is performed, frequency modulated signal is not periodic in the FFT window. Aperiodic situation in the periodic FFT process $(periodicin0 - 2\pi)$ cause to rises in side lobes' magnitude since spectral leakage of harmonics of sinc is rectangular window's frequency response. Rectangular window is the effect of fitting a non-periodic function in the FFT window. By applying other window functions, effects of rectangular window can be reduced, in other words, side lobes are suppressed.

Windowing is used in radar process and helps to reduce amplitude values of side lobes which are undesirable effects and might cause to false alarms. Also, same problem has been tried to be solved by reducing side lobes of antennas by designers. At the first process, side lobes are 13 dB down from the main lobe and second part gives 20 dB differences in amplitude.

Before FFT process, by applying time window like in Hamming schemes, 40-50 dB differences are expected in average of side lobes down below main lobes. The only disadvantage of windowing is broadening of the main lobe.

In the process, Hamming window (Figure 4.8) is used two times. Firstly, before first FFT, M sampled hamming pulse is used on each sweep and secondly, N sampled Hamming window is applied on each columns in the coherent integration [15].

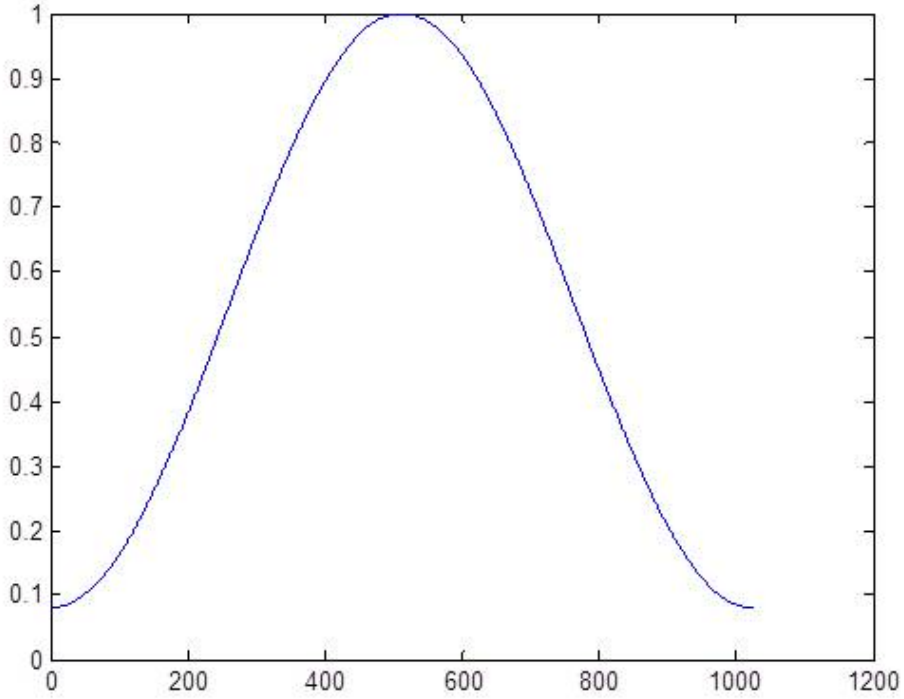

Figure 3.5: Hamming Window.

Table 3.1: Example of FFT windows and highest side lobe level [1].

FFT Window	Highest Side lobe
Bartlett	-26dB
Hanning	- 32 dB
Blackman	-74 dB
Tukey	-13 dB
Hamming	-42dB

Table 3.2 at above, shows FFT window examples which have highest side lobe amplitude.

4. DESCRIPTION OF SIMULATION ALGORITHM AND RESULTS

4.1 Algorithm Overview

This simulator allows investigation in all elevation and azimuth by scanning the environment. First of all input parameters can be examined in two parts, radar and rain parameters. Radar parameters are antenna half power beam width angle, azimuth and elevation angles, antenna gain and pattern, one sweep time, output power, pulse repetition frequency etc. whereas rain parameters are rain drop size distribution, rain rate, drops' radar cross sections, free fall speed and wind velocities.

General flow of algorithm can be explained in the five parts. First step is the construction of observation environment cube. The cube's boundaries are determined by user according to desired observation area and 5 meters margin is added for process of drop replacement which occurred in the every time steps. Also antenna beam resolution area, which indicates radiation field, is formed in the observation cube according to half power beam width, elevation and azimuth angles. Desired observation area is based on antenna radiation beam and margin is added on radiation boundaries. Process runs in the cube, so the cube should be as small as possible for the minimum running time of algorithm.

Second step is creation of rain drops by using Marshal-Palmer Equation and randomly placing in the cube. However M-P equation creates pretty much drops, so number of drops is divided by a norm value and in the algorithm it is chosen as sixth power of ten. This number is decided by considering process time. In this part additionally RCS (radar cross section) values are calculated for each drop.

Third part is picking up the rain drops, which are in the antenna radiation pattern, by using bore sight angle of radar and determined observation range. A matrix having radar cross section values and position data in spherical coordinates is build. And then in-phase and quadrature values of returned signal are calculated.

After calculation of return signal, in the fourth step rain drops are relocated according to fall speed and wind speed in the cube and then loop is turning to third part. In the last part, digital signal processing for getting range and Doppler results.

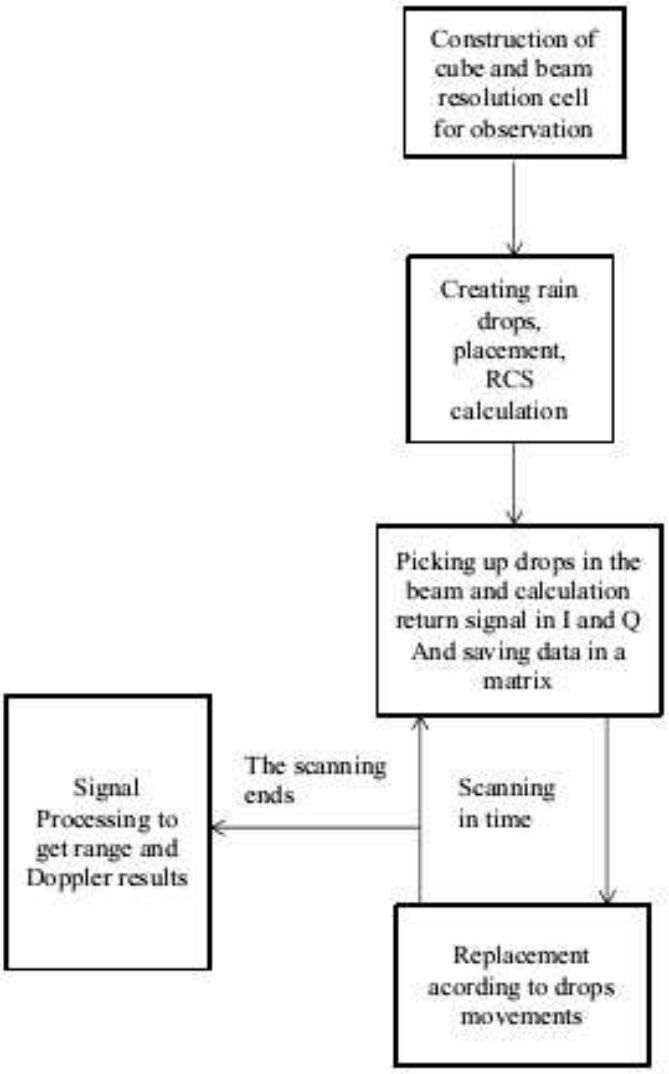

Figure 4.1: Flow Diagram of Algorithm.

In FMCW saw tooth modulation is used in 3 types. Modulation type 3 is normal saw tooth and in this modulation the second beat frequency is occurred as it can be seen in the Figure 3.4. The reason of using different types of modulation is getting rid of the second beat frequency. In the first type, sampling starts at after two way traveling time allowing wave to reach the farthest drop and turn back to radar at the end of the ramp to take same amount of samples from each target. Second type allows the problem of second beat frequency to solve but it causes differences on number of samples between closest drops to radar and farthest drops. In the work, comparing different types of modulations are desired to observe to see effects on the results.

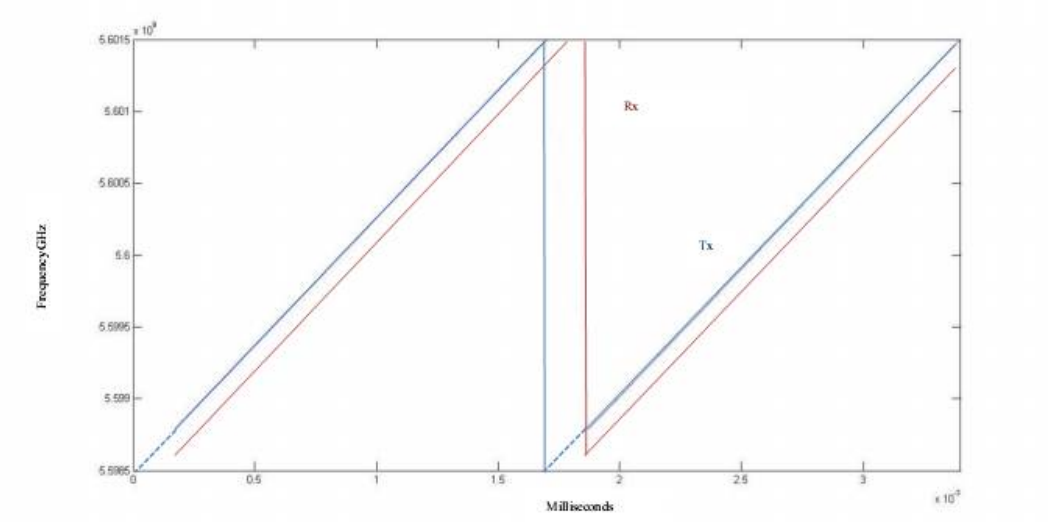

(a) Modulation Type 1 - To get same amount of from every drop, by waiting for the process 2 way time travel to the point of farthest target.

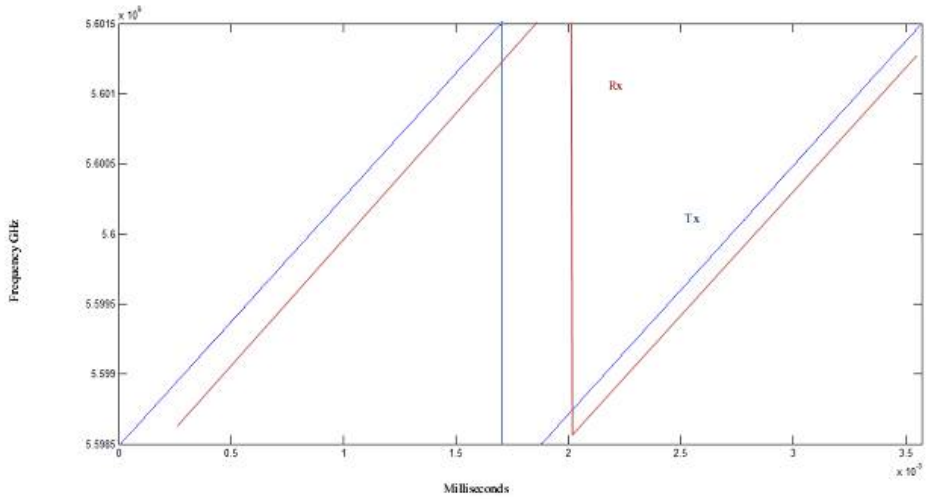

(b) Modulation Type 2 - Transmit signal before each sweep by 2 way time travel to the point of farthest.

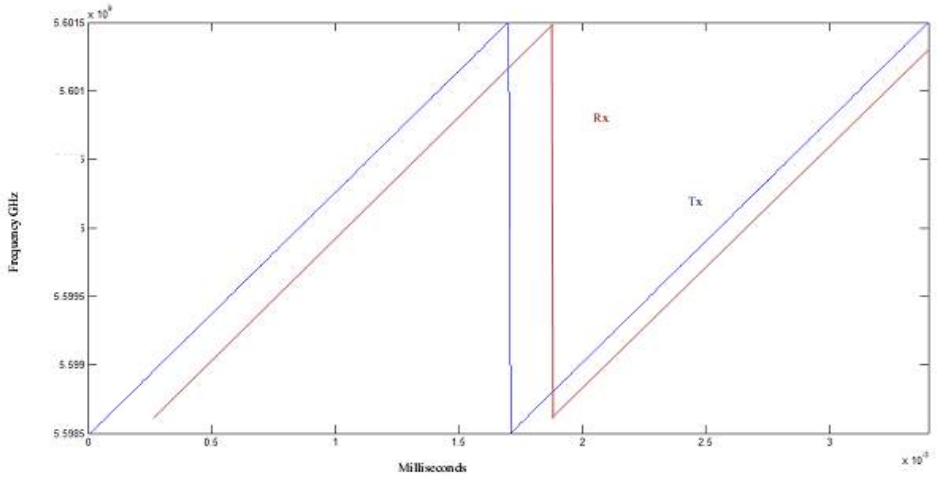

(c) Modulation type 3 - modulation without any waiting time in the transmitting and receiving.

Figure 4.2: FMCW saw tooth modulation types.

4.2 Part 1 - Creating Environment

Construction of observation cube is based on antenna beam cone shape. By using half power beam width angle and considering margin allowing replacement of drops, eight corners position of cubes are determined. The eight points are determined as corners of cube on the antenna beam cone. Then maximum values of x, y and z Cartesian positions of eight points are determined and points are relocated according to max. x, y, z values. And margin is added on x, y and z Cartesian position values. While changing azimuth and elevation angle, also observation cube is relocated because if calculation time is considered, it is not best way to construct fixed cube which allows scanning process in it. By setting cube according to antenna beam, less rain drops are created and replaced. Depth of the cube is determined by maximum range of radar.

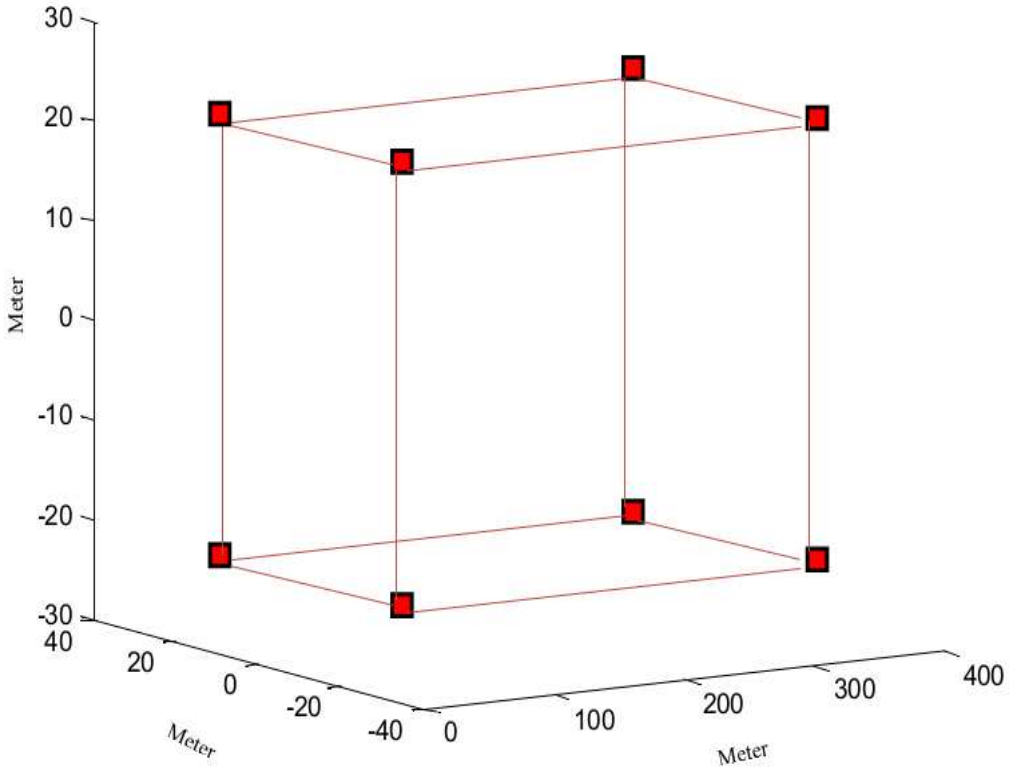

Figure 4.3: Observation cube.

Antenna beam resolution cell is build according to half power beam width and cone shape can be seen at Figure 4.2 showing with rain drops in the beam resolution cell.

4.3 Part 2 - Creating Rain Drop and Locating

In this part, rain drops are created by using Marshall-Palmer drop size distribution. And also diameter resolutions are determined considering the number of small rain drops more than number of bigger drops. First of all minimum drop diameter is 0.5mm and maximum diameter is 8mm. Resolution of drop diameter between 0.5mm and 1mm is 0.08, diameter between 1mm and 5mm is 0.3 and diameter between 5mm and 8mm is 0.8. Then rain drops are randomly located in the cube. Spherical coordinates, diameter, angle which is the angle off bore sight and RCS values of rain drops are saved in a matrix.

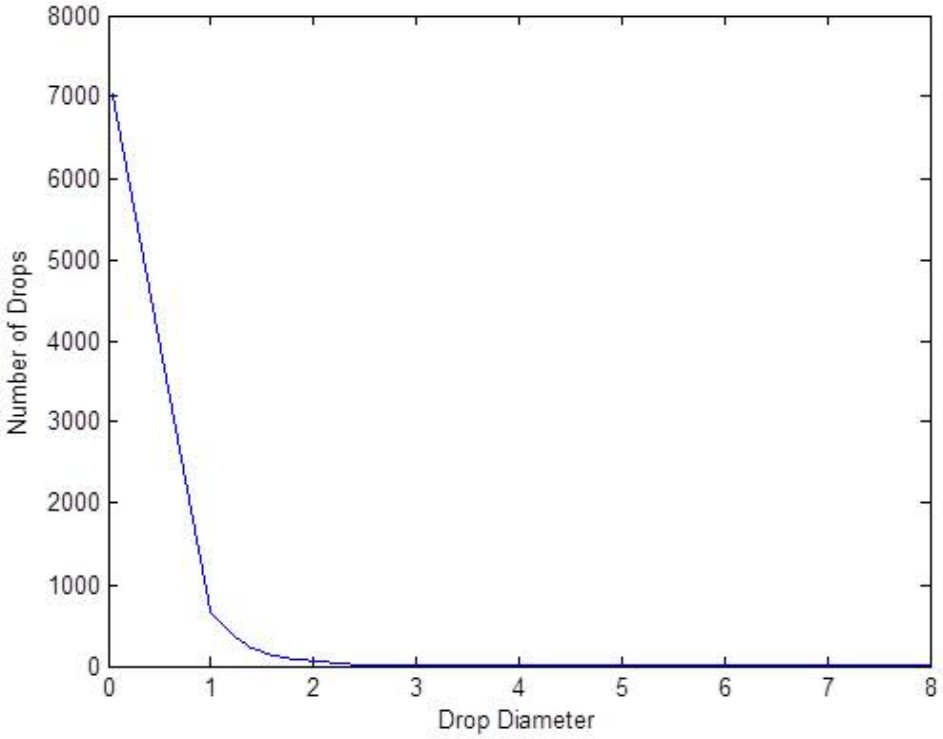

Figure 4.4: Created rain drops diameter and number of drops (M-P).

4.4 Part 3 and 4 - I and Q Calculation

In this section, time and frequency vectors are determined according to modulation type, number of samples in one sweep and number of sweeps in total. In the process loop, rain drops in antenna beam are determined by comparing with bore sight angle and antenna half power beam width angle. Following, in-phase and quadrature values

of returned signal are calculated by using equations 3.9-3.12. Afterwards drops are relocated in the time by using velocity in the all directions and time resolution in the x, y, z Cartesian coordinates.

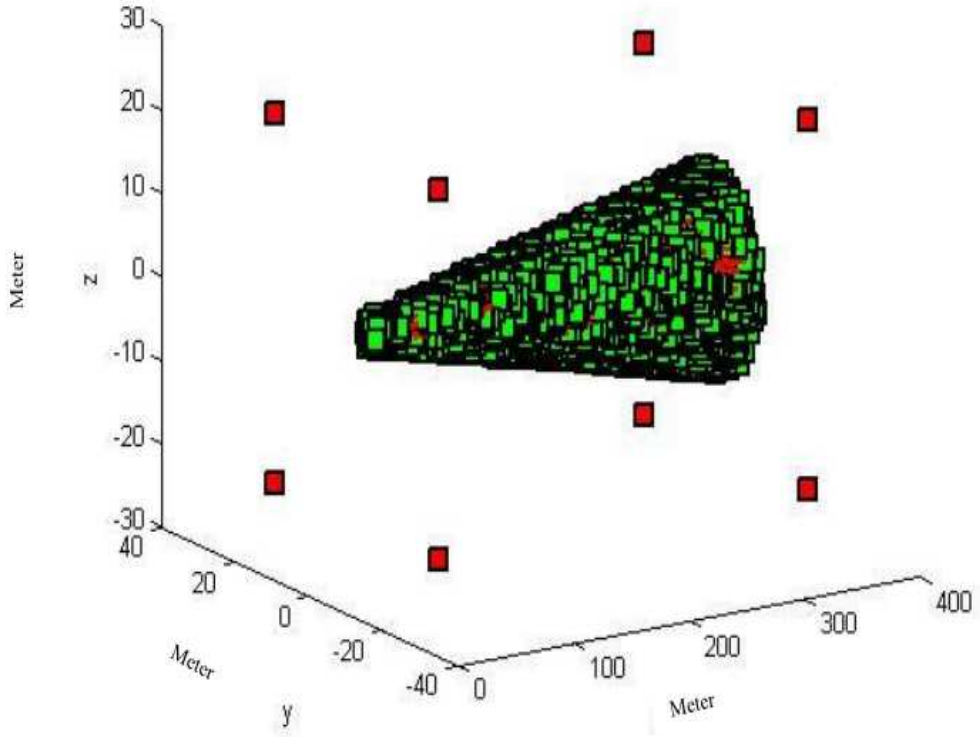

Figure 4.5: Rain drops in the antenna beam.

4.5 Part 5 - DSP

In this part, digital signal processing is carried out. In-phase and quadrature values are collected in 1xM*N sized D vector. M is number of samples in the one sweep and it restricts maximum observation range. N is number of sweeps which restricts Doppler velocity resolution. Next, NxM sized matrix is created from D vector. Suggested by Barricks, 2D FFT process is applied. First FFT are processed over sweeps (rows) which gives range information of targets. Second FFT are applied to get Doppler over columns in the NxM sized matrix of first FFT result. Detailed explanation of signal processing mentioned in the section 3.4.

According to design consideration, required FFT parameters determined and double FFT performed over D where D=I+jQ. M value is equal to 1024 and N value is equal to 128. M is number of samples in one sweep which restrict maximum range and N determines resolution of the Doppler speed. Figure 4.4 is first FFT of data over one

sweep which is received from 500 drops in the range in 3 MHz bandwidth while the range resolution is 50 meters. Number of drops is chosen as 500 because FFT result of precipitation event has a character like noise and 500 drops allow to be seen in the figures. And also process time is considered while deciding number of drops.

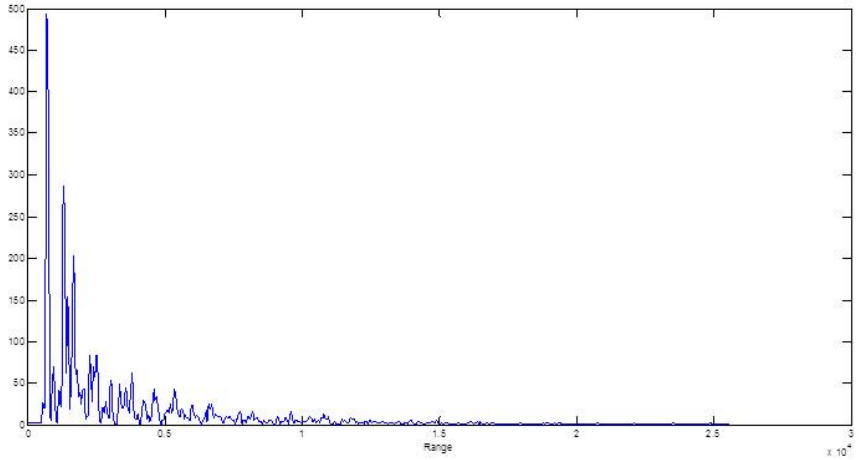

Figure 4.6: First FFT result, range bins and amplitude by 500 drops.

Figure 4.5 displays second FFT over first FFT values as explained in the section 3.4. Second FFT is obtained over column (N column in the result of first FFT). It gives Doppler velocity information and Figure 4.5 is 3D shows Doppler velocity and range together.

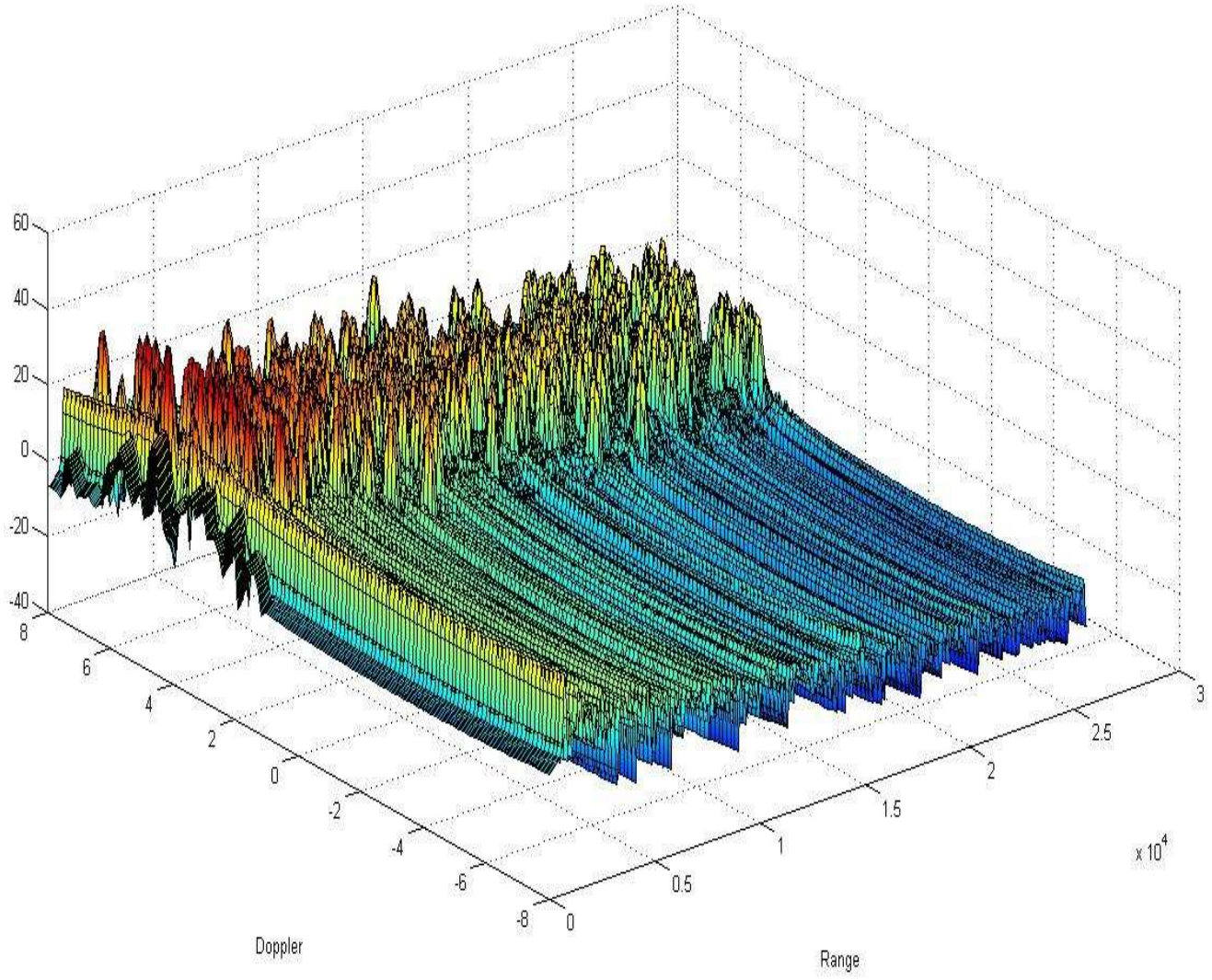

Figure 4.7: With second FFT result in dB Doppler frequency and range by 500 drops.

Table 4.1: Drops Range Data.

Drops	Range [m]	Range calculated by FFT [m]
Drop 1	2067	2100
Drop 2	5926	5950
Drop 3	6233	6250
Drop 4	6617	6650
Drop 5	10150	10200
Drop 6	12478	20900
Drop 7	20862	21000
Drop 8	20980	21800
Drop 9	21748	21800
Drop 10	25238	25300

On the Figure 4.4, it is possible to see that rain events FFT graphic is like noise because of randomly distributed targets. Wind velocity is 4m/s on x axis and spread is 1 m/s. In the figure 4.5 and 4.6 are achieved by using 10 targets to see better the results and with same velocity.

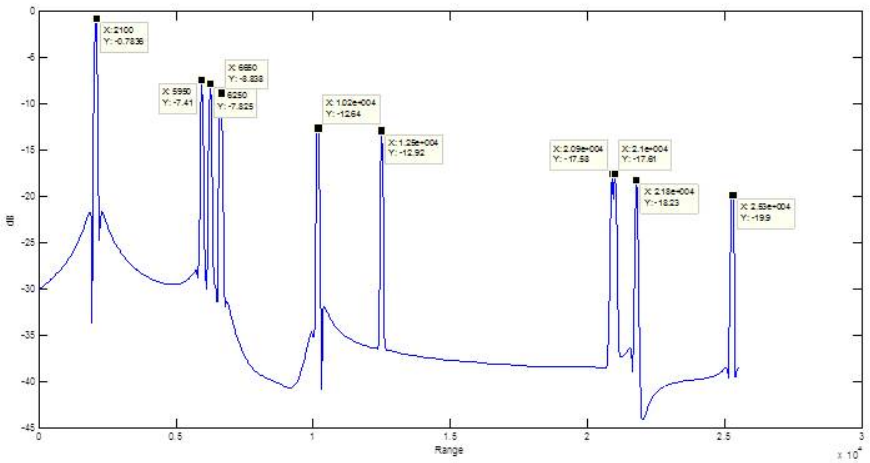

Figure 4.8: First FFT result, amplitude by 10 drop.

In the table 4.1, the real range of rain drops in the simulation reflected respectively and the range is calculated by the FFT and pointer on the Figure 4.5 shows values in range resolutions (50 m).

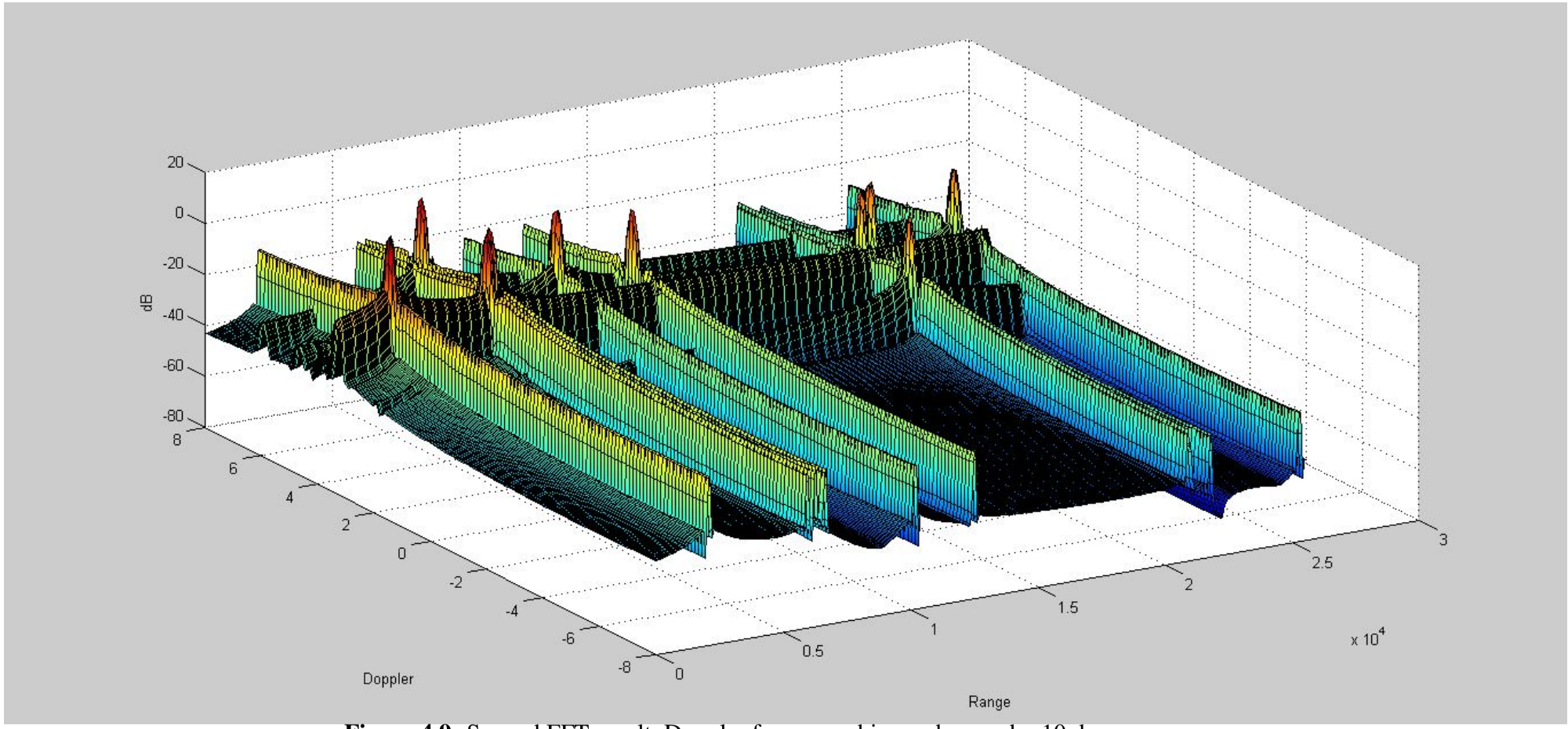

Figure 4.9: Second FFT result, Doppler frequency bins and range by 10 drops.

Table 4.2: Targets Velocity Data.

Drops	Range [m]	Range calculated by FFT [m]
Drop 1	1.7873	1.723
Drop 2	3.2202	3.2
Drop 3	3.2494	3.2
Drop 4	3.5760	3.816
Drop 5	3.7735	3.816
Drop 6	3.9563	3.816
Drop 7	3.9988	4.062
Drop 8	4.1241	4.062
Drop 9	4.5810	4.555
Drop 10	5.8096	4.555

Following graphic (Figure 4.7) shows second FFT result which gives Doppler velocity results and following table gives actual speeds in the direction to antenna and second FFT results. N restricts Doppler velocity resolution and in this case resolution is equal to 0.1213 m/s

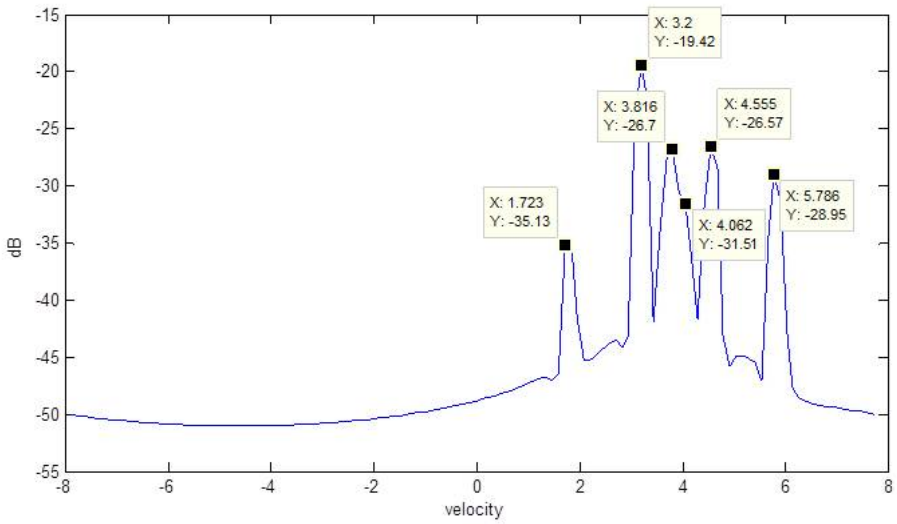

Figure 4.10: Second FFT graphic, Doppler frequency bins and amplitude by 10 drops.

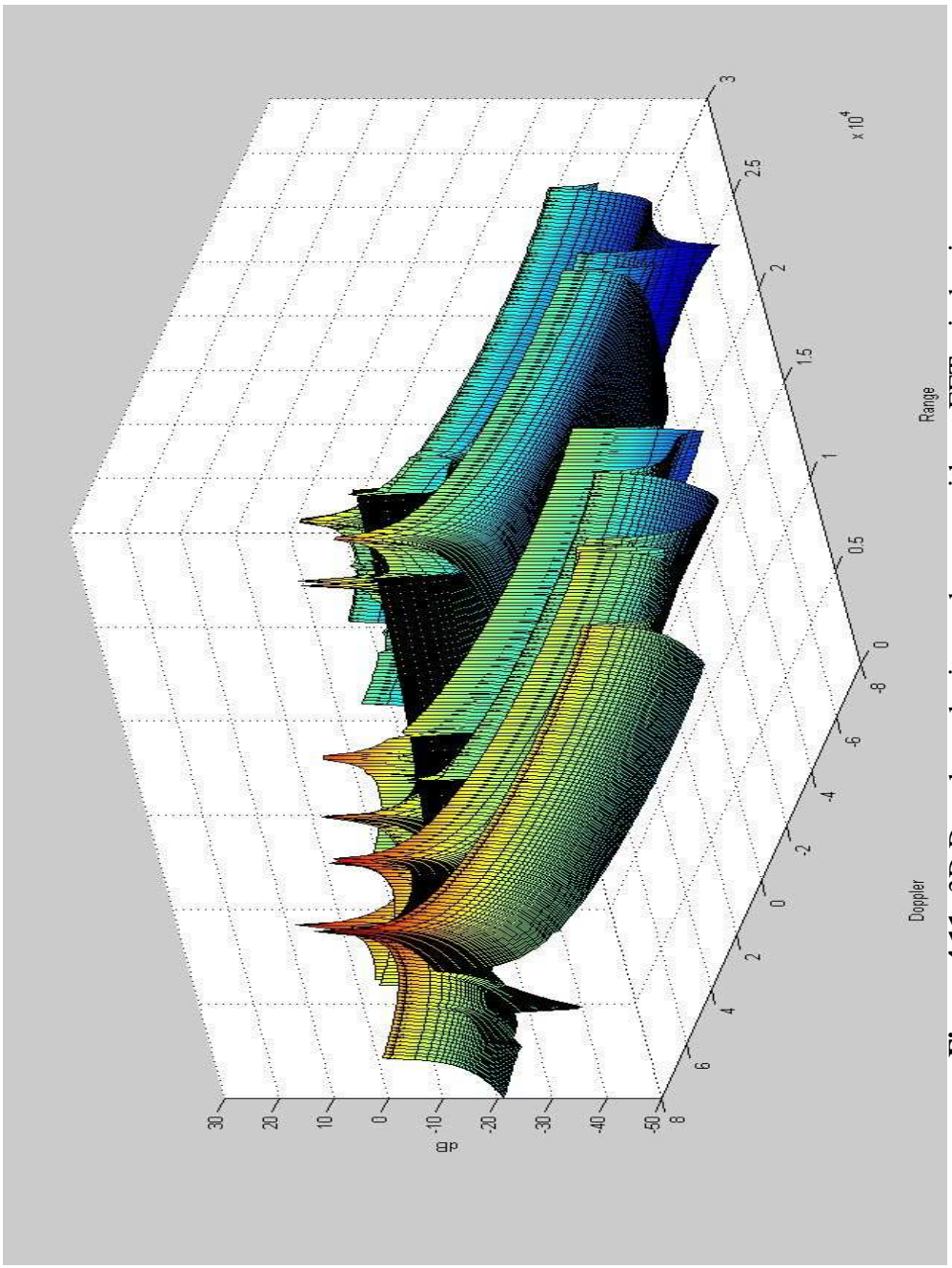

Figure 4.11: 3D Doppler velocity and range without FFT windowing.

By applying window, around 25-35dB differences can be achieved between peaks and side lobes.

Following figures, 4.10, 4.11, 4.12, are results of 3 types of modulation. In first type, it is being taken samples on received signal by waiting for a while which is two way travel duration between radar and target at maximum range. In other words, while radar is working, receiver starts to take samples after wave turned back from farthest target. This method helps to take same amount of samples from each drop in the all range interval (Figure 5.1). Modulation type two (Figure 5.2) is eliminates also second beat frequency by waiting for a while, which is two way travel duration between radar and target at maximum range, before ramps starts. When type 2 is compared with type 1, only difference is that waiting for a while before taking samples (meanwhile transmitter process) in type 1 and in type two receiver stops working until last transmitted frequency turns back from farthest target before starting next ramp. Type 3 (Figure 5.3) is unset saw tooth modulation.

Equation 3.11 is not enough for second beat frequency. In the algorithm following equation, which is get by using equations 7.b and 1 in reference [3], is used in the time interval which second phase (second beat frequency) is occurred.

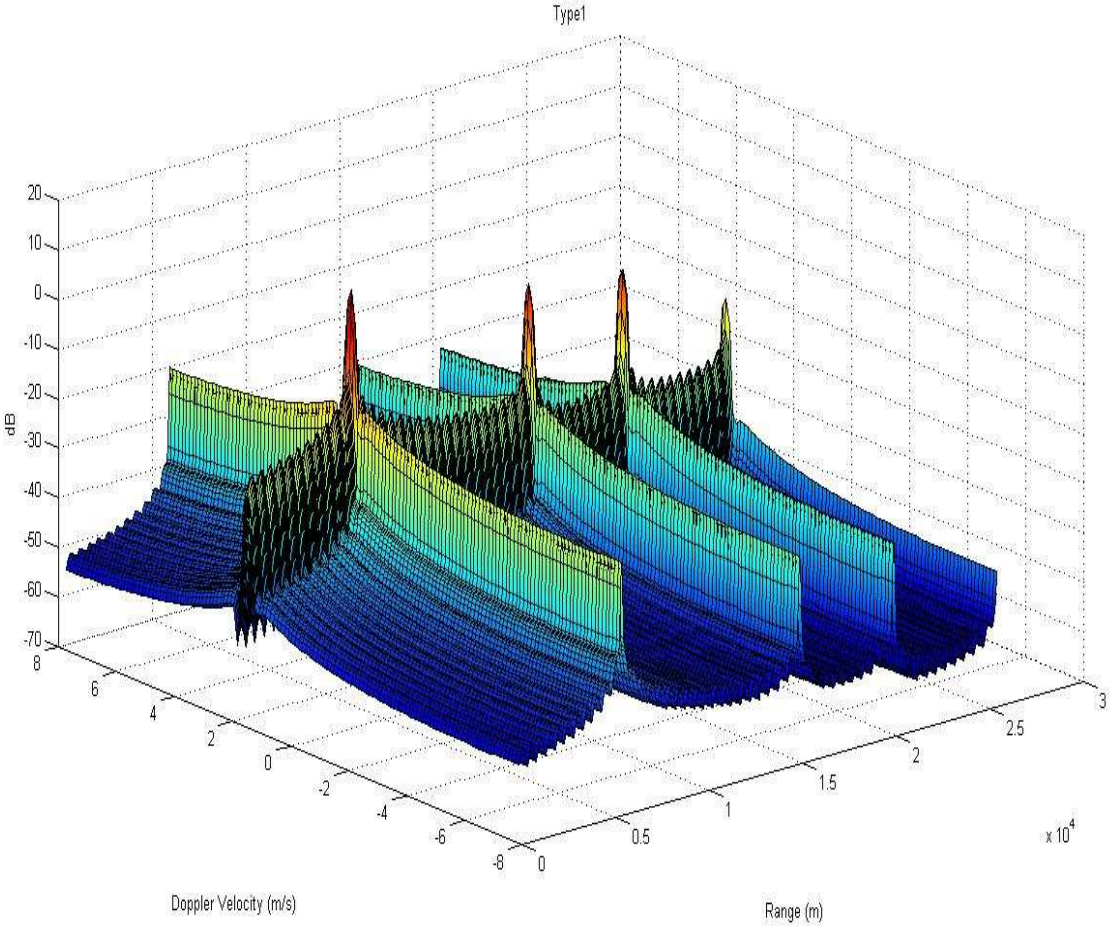

Figure 4.12: Modulation type 1 - Range and Doppler Velocity Ambiguous Function.

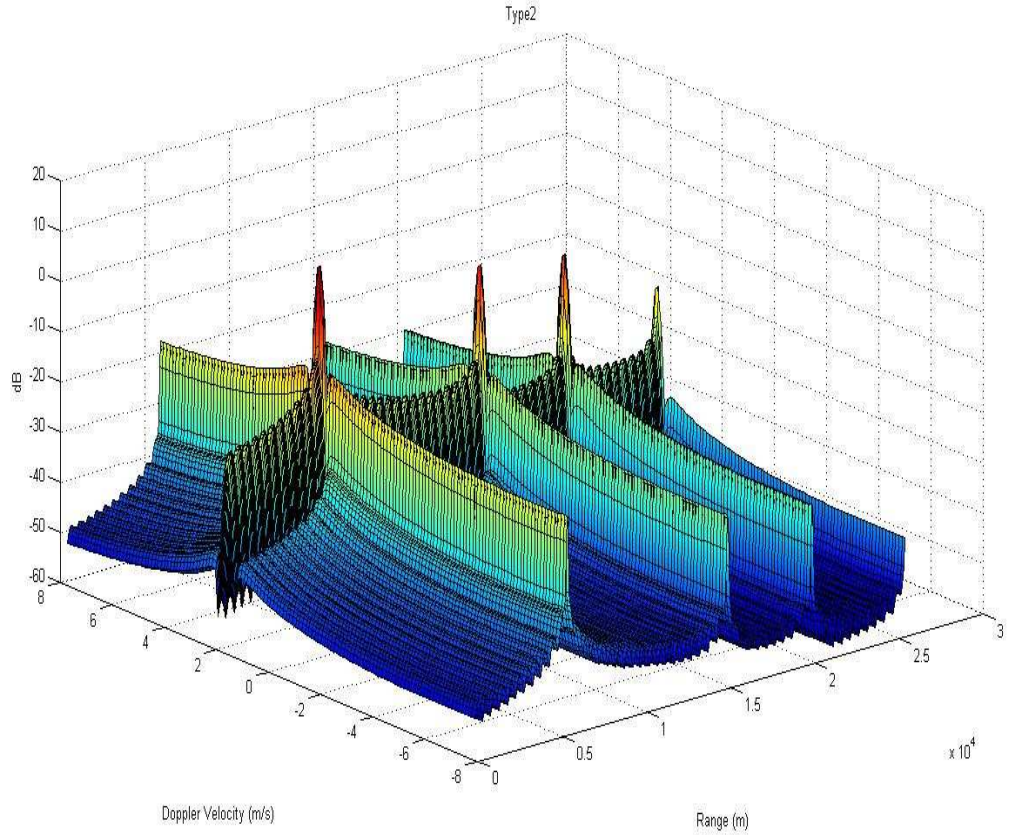

Figure 4.13: Modulation type 2 - Range and Doppler Velocity Ambiguous Function.

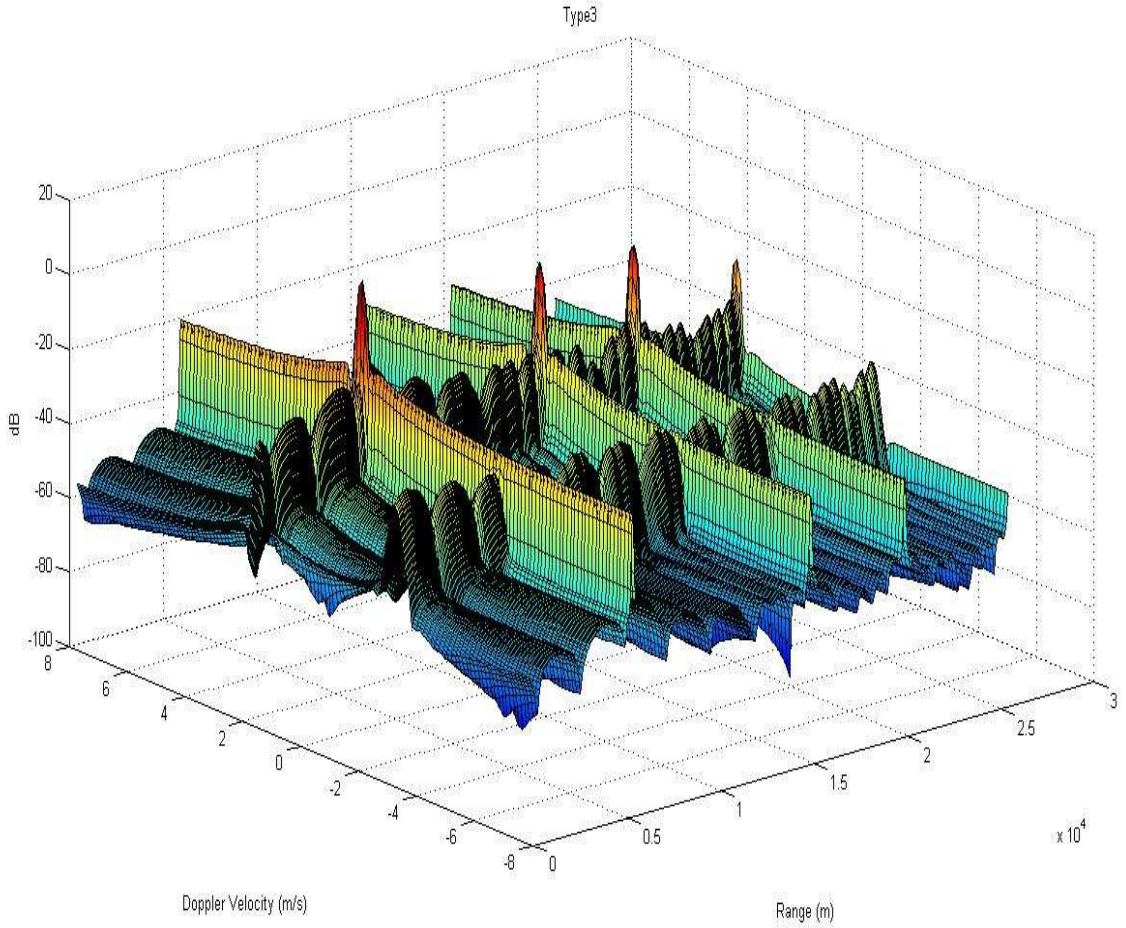

Figure 4.14: Modulation type 3 - Range and Doppler Velocity Ambiguous Function.

Table 4.3: Amplitude values of range-Doppler between Modulation Types.

Modulation	Range [m]	Amplitude [dB]	Side lobe [dB]	
			Doppler	Range
Type 1	5500	12.28	-11.83	-9.745
	15000	3.219	-21.16	-15.58
	20050	0.4404	-23.68	-20.13
	25550	-11.5	-35.58	-21.49
Type 2	5500	11.82	-9.16	-10.41
	15000	2.758	-18.23	-16.16
	20050	-0.1123	-21.01	-20.59
	25550	-11.97	-32.93	-22.2
Type 3	5500	12.35	-11.76	-10.18
	15000	3.249	-23.69	-20.64
	20050	0.4342	-23.95	-20.28
	25550	-11.5	-35.61	-21.82

It can be seen from Table 4.3 that amplitude in dB increases from modulation type 2 to 1. Modulation type 1 aims to solve second beat frequency and take equal amount of sample from every drop. In every sample, information of every drop is included and this leads to increase in amplitude. Type 2 also clears second beat frequency but it can be seen from Figure 4.14 that type 3 cause unwanted signals on the Range-Doppler map. Additionally, from type 2 to 1, side lobe improvement can be seen. Fluctuation (or periodicity) on side lobe is related with bandwidth. In type 2 and type 1, some part of sample in the ramp is ignored and it makes relatively bandwidth decrease. That's why there is difference on side lobe periodicity between type 2 or 1 and 3.

Also Figure $4.A1 - 4.A3$ show Doppler - Range ambiguity in the situation of different velocities targets have. Targets have 4 m/s to 1 m/s velocities respectively.

5. CONCLUSION

By developing digital signal processing algorithm for rain form of precipitation by using Frequency Modulation Continues Waves (FMCW), it is aimed to observe precipitation behavior and calculate returned signal strength from randomly distributed volume target, range and velocity of every drop. In the algorithm, firstly target volume is created by considering calculation time and enabling drops to fall in antenna beam resolution volume in time. Using Marshal-Palmer drop size distribution, rain drops are created and located randomly in the volume. Then rain drops in the antenna beam resolution volume are chosen and radar cross section values are calculated considering Rayleigh scattering region.

Operating frequency is determined to be 5.6 GHz since targets fall into Rayleigh scattering region when frequency and target size are compared (ten times smaller than wavelength). Terminal velocity of drops are calculated by Atlas et Al.'s equations which give relation drops diameter and terminal velocity. Antenna half power beam degree is decided as 4 degree but antenna and the other parameters like rain rate can be determined and changed according to process.

By using position of rain drops in the antenna beam resolution and their velocity, phase values are determined and RCS, distance, pulse width, frequency and other related parameters and I (phase) and Q (quadrature) components of received signal are calculated. These components can be used to investigate reflectivity, velocity of targets and velocity spread. First and second Fast Fourier Transform (FFT) is implemented for range and velocity information.

Algorithm allows the investigation area to be defined by user in range, elevation and azimuth. The box, which is target volume, has 5 meter margin in addition to antenna beam being observation area.

Rain rate value in the results is 10 [mm/hr], which is always same in different observation areas. Normally, it should be scaled according to observation volume and

norm value should be used to reduce number of drops for decreasing calculation time. Scaling is not used because rain rate value (10 mm/hr) already provides around 8000 drops since this study is held by using computer which has Intel core i5 CPU M 460 2.53 GHz and 3 GB ram.

In the previous section the effect of the windowing was proved by comparing values of real range and velocity parameters in first FFT and second FFT results. Effects of modulation type can be seen from Table 4.3 that amplitude in dB increases from modulation type 2 to 1. Modulation type 1 aims to solve second beat frequency and take equal amount of sample from every drop. In every sample, information of every drop are included and this leads to increase in amplitude. Type 2 also clears second beat frequency but it can be seen from Figure 4.14 that type 3 cause unwanted signals on the Range-Doppler map. On side lobes, improvement can be seen by comparing type 2 and 1.

Figure 2.7 is result of Hamming window function application and Figure 2.10 reflects the result without FFT windowing. Difference between main lobes and side lobes should increase around 25 dB, but when Figure 2.7 and Figure 2.10 compared, the difference is about 12 dB without windowing and 34 dB with windowing between main lobes and side lobes. So improvement on the lobes difference is around 22dB.

For the gain of the thesis, it can be seen that I and Q formulation for pulse Doppler radar simulation works for FMCW. By using 2D FFT method, Doppler velocities and range values of distributed targets can be achieved and efficiency of FFT windowing is approved. Additionally, it is seen that second beat frequency problem for saw tooth modulation can be solved by setting transmitting time and time of taking samples on frequency ramp.

REFERENCES

[1] **Url-1**, http://www.physik.uni-wuerzburg.de/~praktiku/Anleitung/Fremde/ANO14.pdf, date retrieved 12.08.2013.

[2] **Url-2**, http://en.wikipedia.org/wiki/File:Doppler_effect_diagrammatic.png, date retrieved 03.05.2013.

[3] **Barrick, D.E.**, FM/CW Radar Signals and Digital Processing, NOAA Technical Report ERL 283-WPL 26.

[4] **Capsoni, C. and Amico, M.** (1998). A Physically Based Radar Simulator, *Atmospheric and Oceanic Technology*, 593–598.

[5] **Doviak, R.J. and Zrnic, D.S.**, (1984). Doppler Radar and Weather Observations, Academic Press, 2. edition.

[6] **Schroder, U.P.** (2005). Development Of A Weather Radar Signal Simulator To Examine Sampling Rates And Scanning Schemes, *Ph.D. thesis*.

[7] **Skolnik, M.**, (2003). Introduction to Radar Systems, McGraw-Hill Education, 3. edition.

[8] **Url-3**, http://www.physik.uni-wuerzburg.de/~praktiku/Anleitung/Fremde/ANO14.pdf, date retrieved 12.08.2013.

[9] **Leuenberger, A.** (2009). Precipitation Measurements with Microwave Sensors, *Ph.D. thesis*.

[10] **Yuter, S.E. and Hagen, M.** Relations between radar reflectivity, liquid-water content, and rainfall rate during the MAP SOP, *Q. J. R. Meteorol. Soc.*, ***129***.

[11] **Pruppacher, H. and Beard, K.V.** A wind tunnel investigation of the internal circulation and shape of water drops falling at terminal velocity in air, *Q. J. R. Meteorol. Soc.*, ***96***.

[12] **Williams, C.R. and Gage, K.S.** Raindrop size distribution variability estimated using ensemble statistics, *Ann. Geophys.*, ***27***.

[13] **Atlas, D.**, **Srivastava, R.C. and Sekhon, R., S.** Doppler radar characteristics of precipitation at vertical incidence, *Geophys. Space Phys.*

[14] **Harikumar, R.** (2009). Study on tropical rain with special reference to rain Drop Size Distribution and integral rain parameters using ground-based and satellite measurements, *Ph.D. thesis*, Department of Physics, Cochin University of Science and Technology, India.

[15] **Balanis, C.B.**, (2005). Antenna Theory: Analysis and Design, John Wiley Sons.

APPENDICES

APPENDIX A : Figures

APPENDIX A

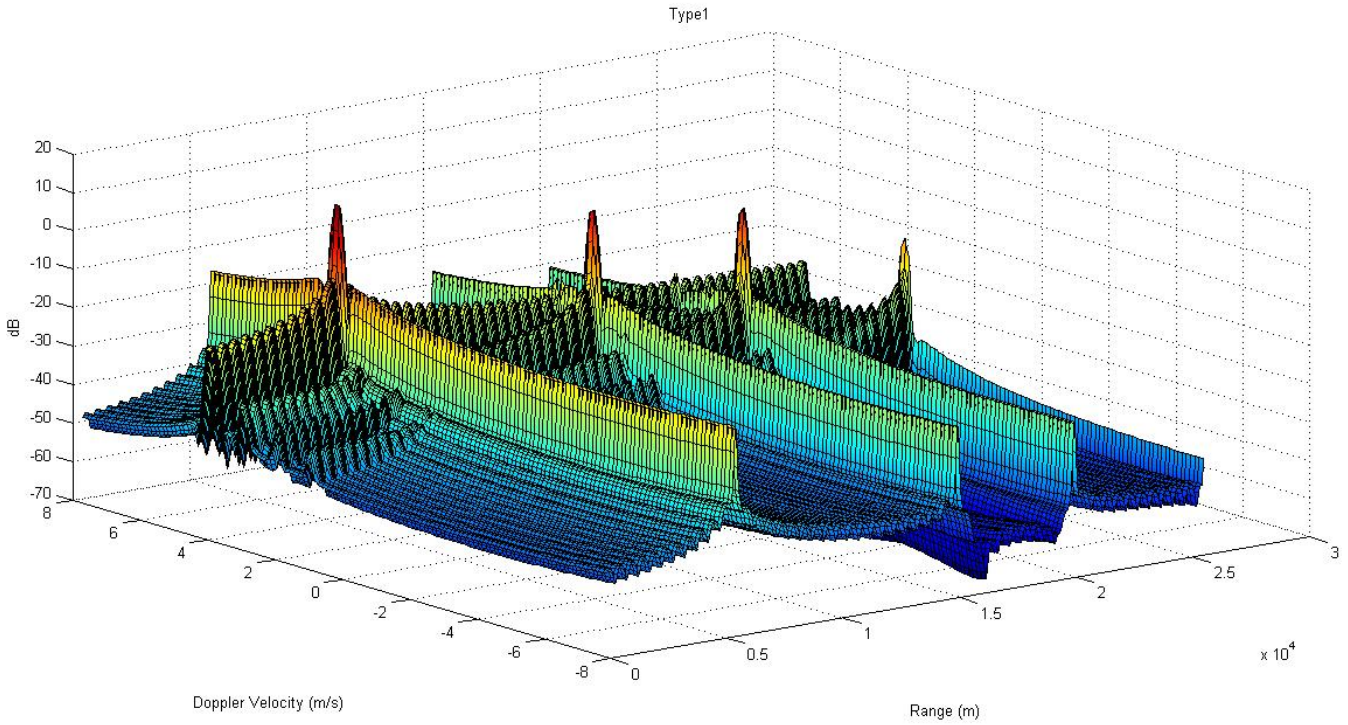

Figure A.1: Modulation type 1 - Range and Doppler Velocity Ambiguous Function in Different Velocities.

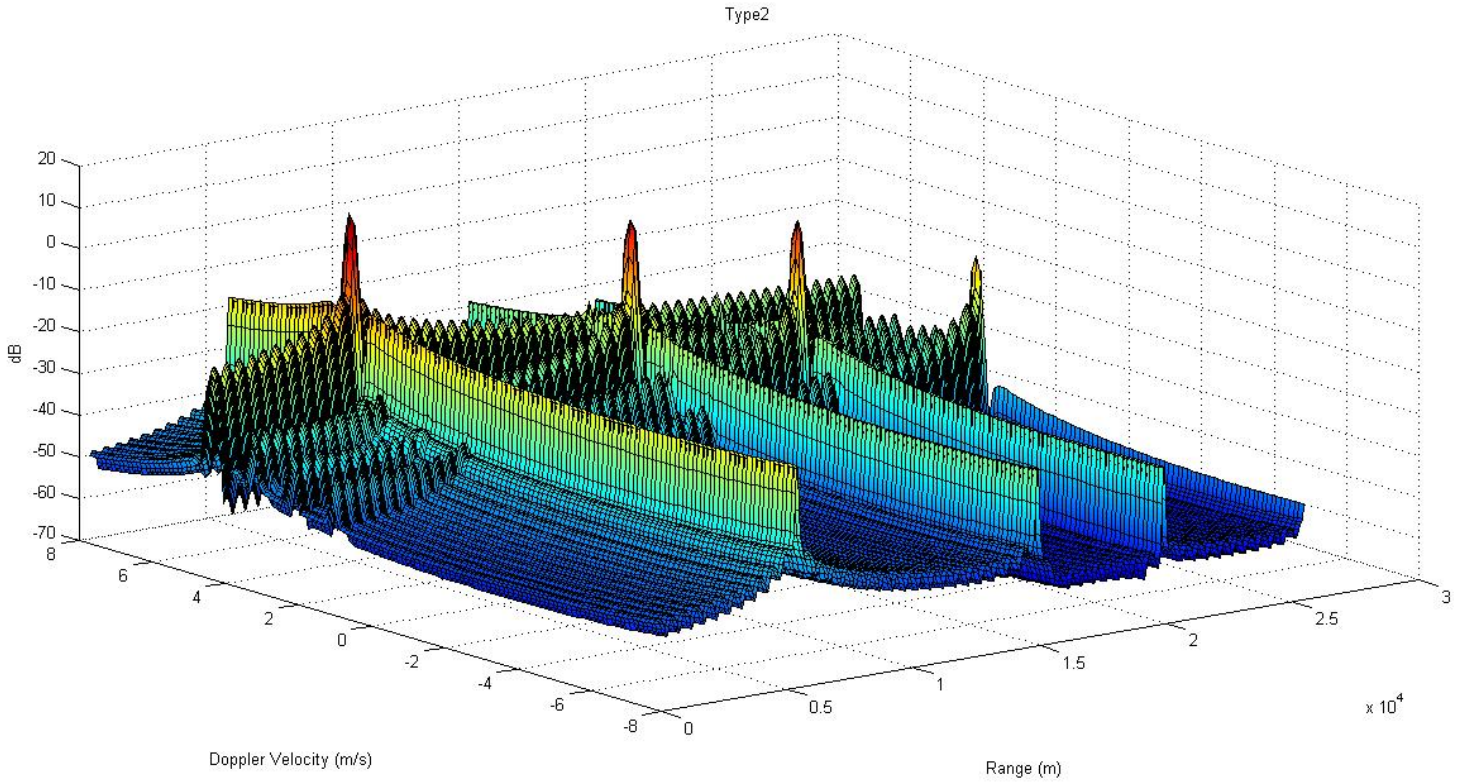

Figure A.2: Modulation type 2 - Range and Doppler Velocity Ambiguous Function in Different Velocities.

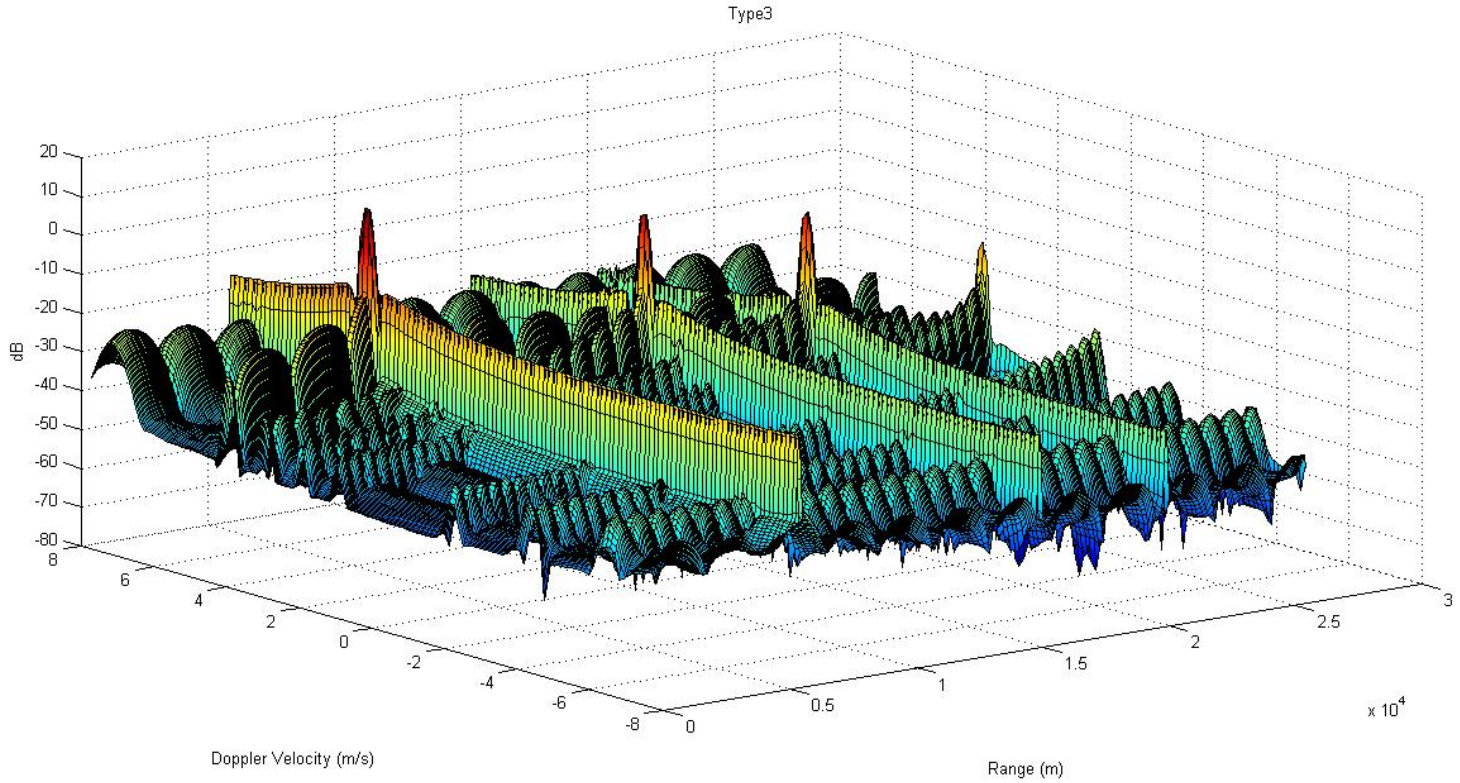

Figure A.3: Modulation type 3 - Range and Doppler Velocity Ambiguous Function in Different Velocities.

Table A.1: Amplitude values of range-Doppler between Modulation Types.

Modulation	Range [m]	Amplitude [dB]
Type 1	5500	11.22
	15000	2.574
	20050	0.3812
	25550	-10.95
Type 2	5500	11.05
	15000	2.876
	20050	0.5423
	25550	-10.91
Type 3	5500	11.29
	15000	2.523
	20050	0.2406
	25550	-10.95

CURRICULUM VITAE

Name Surname:Hasan Isel

Place and Date of Birth:Denizli / 21.06.1988

E-Mail:iselh@itu.edu.tr

B.Sc.: Telecommunication Engineering, Istanbul Technical University

M.Sc.: Telecommunication Engineering Master Programme, Istanbul Technical University

List of Publications and Patents:

Katircioglu, O., Isel, H., Ceylan, O., Taraktas, F., Yagci, H.B., Comparing Ray Tracing, Free Space Path Loss and Logarithmic Distance Path Loss Models in Success of Indoor Localization with RSSI, 19th Telecommunication Forum (TELFOR 2011), Nov. 22-24, 2011, Belgrade/Serbia

Ceylan, O., Yilmaz, O., Isel, H., Yagci, H.B., Aslan, A.R., Antenna Design and Deployment Analyses for Turksat-3USAT, 3rd Nano-Satellite Symposium, Dec. 12-14, 2011, Kitakyushu / Japan

Isel, H., Kurt, Y., Yilmaz, O., Furkan, A. T., Ceylan, O., Yagci, H. B., 435 MHz Monopole Antenna Design for Turksat-3USAT Nano Satellite, IEEE 19. Sinyal Isleme ve Iletisim Uygulamalari Kurultayi (SIU 2011), 20-22 Nisan 2011, Antalya.